Spreading of the Western Mediterranean Deep Water after winter 2005: Time scales and deep cyclone transport.

Jonathan Beuvier, K. Béranger, Cindy Lebeaupin Brossier, Samuel Somot, Florence Sevault, Yann Drillet, Romain Bourdallé-Badief, Nicolas Ferry, Florent Lyard

Spreading of the Western Mediterranean Deep Water after winter 2005: Time scales and deep cyclone transport

J. Beuvier,[1,2,3] K. Béranger,[2] C. Lebeaupin Brossier,[2,3,4] S. Somot,[3] F. Sevault,[3] Y. Drillet,[1] R. Bourdallé-Badie,[1] N. Ferry,[1] and F. Lyard[5]

Received 11 October 2011; revised 29 May 2012; accepted 4 June 2012; published 26 July 2012.

[1] This work is dedicated to the study of the propagation of the Western Mediterranean Deep Water (WMDW) formed in the Gulf of Lions during the exceptional winter 2005. A simulation of the 1998–2008 period has been carried out with an eddy-resolving Ocean General Circulation Model of the Mediterranean Sea, driven by interannual high-resolution air-sea fluxes. This study first presents a validation of the recently improved model configuration against satellite observations. Then, we assess the ability of the model to reproduce the particularly intense deep convection event of winter 2005 in the Gulf of Lions. A huge volume of very dense water is formed in the simulation at that time (annual formation rate higher than 3 Sv). The thermohaline characteristics of the new WMDW allow a monitoring of its deep propagation. We identify several deep cyclones as mainly responsible of the fast spreading of the WMDW southwards in the Western Mediterranean. By comparing Eulerian and Lagrangian approaches, we estimate different transport times of the WMDW by these cyclonic eddies and compare them to those deduced from several observations. Finally, we argue that these cyclones favor the propagation of the WMDW thermohaline characteristics toward the Channel of Sardinia and decrease the volume of WMDW which can reach the Strait of Gibraltar.

Citation: Beuvier, J., K. Béranger, C. Lebeaupin Brossier, S. Somot, F. Sevault, Y. Drillet, R. Bourdallé-Badie, N. Ferry, and F. Lyard (2012), Spreading of the Western Mediterranean Deep Water after winter 2005: Time scales and deep cyclone transport, *J. Geophys. Res.*, *117*, C07022, doi:10.1029/2011JC007679.

1. Introduction

[2] Deep convection occurs in the Mediterranean Sea, in particular in the Gulf of Lions in the Western Mediterranean (GoL in Figure 1a). In this particular place, the formation of deep water is mainly triggered by the atmosphere with strong local winds, which lead to a high latent heat loss for the sea [*Schott et al.*, 1996], and by a topographic control [*Madec et al.*, 1996]. The formation process was well described by [*Marshall and Schott*, 1999] in three phases: the preconditioning, the convection and the spreading. The particular circulation through a cyclonic gyre in the Gulf of Lions is enhanced in winter by the winds channeled by the Alps, the Massif Central and the Pyrenees. In the center of this relatively closed gyre, above which strong heat loss occurs, is formed the Western Mediterranean Deep Water (WMDW) in winter. The WMDW plays a major role in the thermohaline circulation of the Mediterranean. This water mass is characterized by a density above 29.10 $kg.m^{-3}$ [*MEDOC Group*, 1970]. The convection regularly reaches the sea bottom, which is about 2400 m depth in this area, and occurs around the 42°N−5°E position, as observed for example in 1982 [*THETIS Group*, 1994].

[3] High resolution ocean modeling studies have proved their skill to accurately reproduce the convection process, at basin scale [*Pinardi and Masetti*, 2000; *Castellari et al.*, 2000; *Artale et al.*, 2002; *Béranger et al.*, 2005; *Fernàndez et al.*, 2005; *Somot et al.*, 2006; *Sannino et al.*, 2009; *Beuvier et al.*, 2010; *Herrmann et al.*, 2010] or at regional scale in embedded models [*Mantziafou and Lascaratos*, 2004; *Herrmann and Somot*, 2008; *Herrmann et al.*, 2008]. In these modeling studies, the atmospheric resolution was proved to be of high importance to allow the simulation of the deep convection without some artificial added forcings. In particular, the wind channeling is one of the main factor that helps the preconditioning phase [*Béranger et al.*, 2010], in producing extreme heat loss [*Herrmann and Somot*, 2008].

[1]Mercator Océan, Ramonville St-Agne, France.
[2]Ecole Nationale Supérieure de Techniques Avancées ParisTech–Unité de Mécanique, Palaiseau, France.
[3]Centre National de Recherches Météorologiques–Groupe d'Etude de l'Atmosphère Météorologique, URA Météo-France/CNRS, Toulouse, France.
[4]Laboratoire de Météorologie Dynamique, Institut Pierre Simon Laplace, Ecole Polytechnique, ENS, UPMC, CNRS, Palaiseau, France.
[5]Laboratoire d'Etudes en Géophysique et Océanographie Spatiales, Observatoire Midi-Pyrénées, UMR CNES/CNRS/IRD/UPS, Toulouse, France.

Corresponding author: J. Beuvier, Mercator Océan, Parc Technologique du Canal, 8-10 rue Hermès, FR-31520 Ramonville St-Agne, France. (jonathan.beuvier@mercator-ocean.fr)

0148-0227/12/2011JC007679

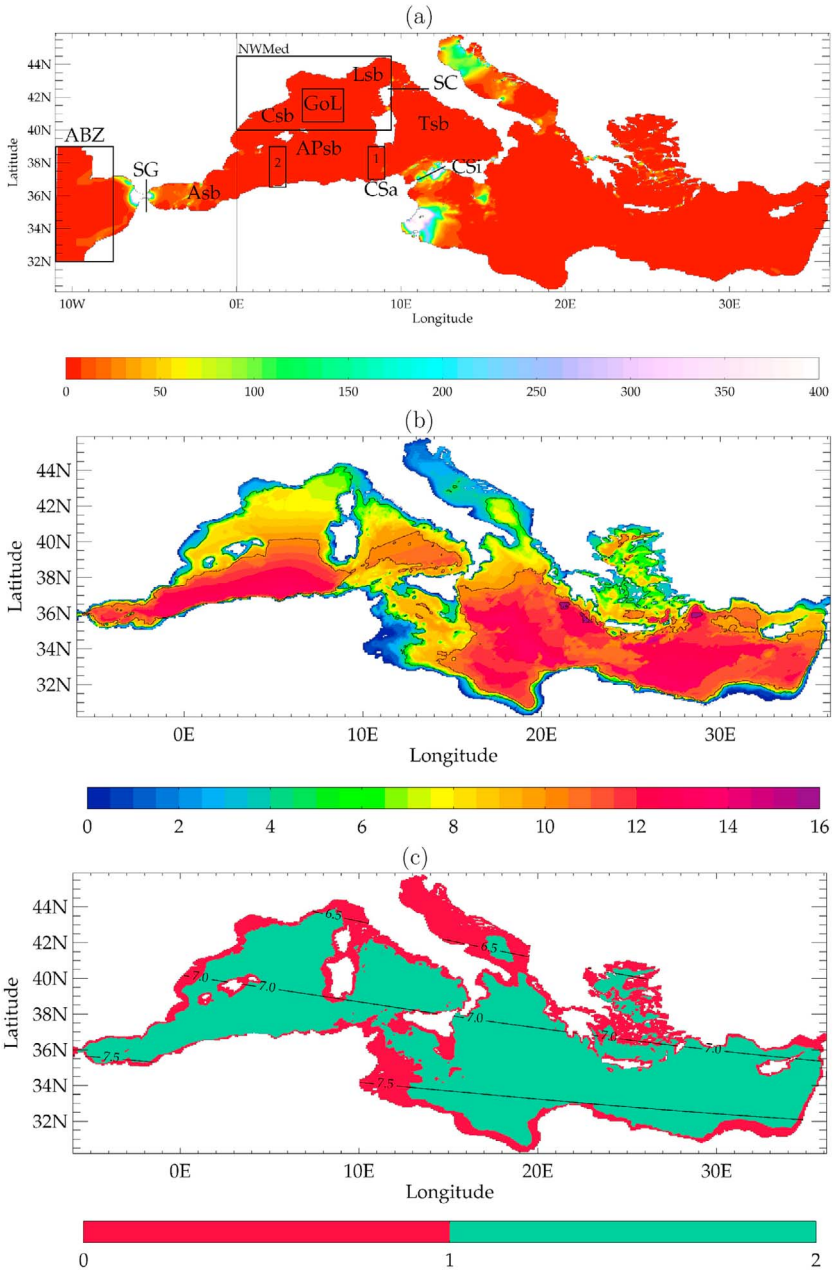

Figure 1. (a) The domain of the MED12 model is illustrated by the bottom turbulent kinetic energy background E ($cm^2.s^{-2}$). This field has a maximum value over 10000 $cm^2.s^{-2}$ at the Strait of Gibraltar. ABZ: Atlantic Buffer Zone, SG: Strait of Gibraltar, CSa: Channel of Sardinia, CSi: Channel of Sicily, SC: Strait of Corsica, GoL: Gulf of Lions, Asb: Alboran subbasin, APsb: Algero-Provencal subbasin, Csb: Catalan subbasin, Lsb: Ligurian subbasin and Tsb: Tyrrhenian subbasin. The Algerian subbasin, when mentioned in the text, corresponds to the southern part of APsb. The rectangle in the northwestern Mediterranean is the area where SSH is averaged in section 3.2. The rectangle in the Gulf of Lions is the area where the density profiles are averaged in section 3.3. The rectangles 1 and 2 are the boxes of the θ-S diagrams in section 4.2. (b) First Rossby radius of deformation (km, contours every 5 km), computed from the MEDATLAS database state representative of the end of the 1990's [*MEDAR/MEDATLAS Group*, 2002], which is the initial state of the simulation performed in this study, and from the bathymetry of MED12. (c) Ratio (in color) between the first Rossby radius of deformation (Figure 1b) and the horizontal grid cell size of MED12 (km, contours every 0.5 km). Values above 1 (in green) show the eddy-resolving domain while some small areas with lower values (in red) characterize areas of well-known low stratification and/or low depth (mainly in coastal areas).

[4] During the winter 2005, a drastic convection event occurred in the Gulf of Lions [*López-Jurado et al.*, 2005; *Schröder et al.*, 2006; *Canals et al.*, 2006; *Font et al.*, 2007; *Smith et al.*, 2008; *Schroeder et al.*, 2008]. Before the event, the previous WMDW has characteristics ranging in 12.75–12.92°C for potential temperature, in 38.41–38.47 psu for salinity and in 29.09–29.10 kg.m^{-3} for potential density [see also *Pinot et al.*, 2002; *Pascual et al.*, 2002]. After the event, the new WMDW potential temperature ranges between 12.87 and 12.90°C, and, the new WMDW salinity ranges between 38.47 and 38.50 psu. The new WMDW has thus a well marked thermohaline signature, as it is saltier and slightly warmer than the previous one, with a corresponding density range of 29.11–29.13 kg.m^{-3}. The formation rate of new WMDW was particularly high compared to other years. *Schroeder et al.* [2008] proposed a value of 2.4 Sv for the two winters 2005 and 2006, while previous estimates are ranged for observations between 0.1 and 1.2 Sv [*Schott et al.*, 1996; *Marshall and Schott*, 1999] and for models between 0.2 and 1.6 Sv [*Castellari et al.*, 2000; *Somot et al.*, 2006; *Béranger et al.*, 2009]. An estimate of its time scale spreading in the Western Mediterranean can be made: the new WMDW thermohaline signature was then detected in the Strait of Gibraltar (SG in Figure 1a) and in the Channel of Sardinia (CS in Figure 1a) by deep observations in 2006. *Schroeder et al.* [2008] argued that it takes less than a year and a half to this new WMDW to spread in the basin, approximately until 3°W. But because the authors used only bi-annual sections in the basin, we do not know too much on the processes involved in this very fast spreading of new WMDW. *Testor and Gascard* [2003] and *Testor and Gascard* [2006], using Lagrangian floats during 1994–1995 and 1997–1998, have shown that submesoscale coherent vortices with a typical size of 5–10 km are one of the involved processes. They estimate that such eddies account for as much as 40% of the new WMDW spreading away from the convection area. With a coastal eddy-resolving model of the Gulf of Lions, *Herrmann et al.* [2008] have highlighted that about one third of the deep water advection after the convection event is made southwestward by very energetic mesoscale structures with a typical size of 25–50 km.

[5] *Herrmann et al.* [2010] have studied the convection phase of the winter 2005 event and its atmospheric and oceanic preconditioning factors. We here investigate the spreading phase of WMDW in winter 2005 to evaluate how the WMDW can be transported from the Gulf of Lions toward the southern channels and at what time scale. We want to complete the fragmented view of this spreading given by the observations of *Testor and Gascard* [2003], *Testor and Gascard* [2006] and *Schroeder et al.* [2008], by using the high-resolution 4D view offered by an ocean model. We use an eddy-resolving model, described in section 2), to study the winter 2005. The formation of WMDW during winter 2005 is first assessed in the model simulation in section 3. Then the spreading phase is studied using Eulerian and Lagrangian diagnostics in section 4. Section 5 is devoted to a conclusion.

2. Model Configuration and Simulation

[6] We use the ocean general circulation model NEMO [*Madec and the NEMO Team*, 2008] in a regional configuration of the Mediterranean Sea called MED12 [*Lebeaupin Brossier et al.*, 2011, 2012]. The development of MED12 is made in the continuity of the evolution of the French modeling of the Mediterranean Sea, following OPAMED16 [*Béranger et al.*, 2005], OPAMED8 [*Somot et al.*, 2006] and NEMOMED8 [*Beuvier et al.*, 2010]. We described here the configuration of the 10-year simulation, named MED12-ARPERA, which will be used in this study.

2.1. Grid and Bathymetry

[7] MED12 covers the whole Mediterranean Sea plus a buffer zone including a part of the near Atlantic Ocean (Figure 1a). It does not cover the Black Sea. The resolution of the horizontal grid of MED12 varies in latitude and ranges between 6.5 and 8 km from 46°N to 30°N (i.e., equivalent to a real resolution between 1/14° and 1/18°, from South to North). In longitude, the horizontal resolution ranges between 5.5 and 7.5 km; these changes in resolution are due to the use of the standard three-polar ORCA grid of NEMO at 1/12°, which is stretched toward a pole located in central Russia, the other two poles being located in north Canada and in Antarctica (South Pole).

[8] MED12 has 50 vertical stretched z-levels (from Δz = 1 m at the surface to Δz = 450 m at the bottom, with 35 levels in the first 1000 m). The bathymetry comes from the 10th version of the MERCATOR-LEGOS bathymetry at a resolution of 30″ × 30″, composed of merging between the GEBCO-08 database, the MEDIMAP bathymetry [*Medimap Group*, 2005] and the Ifremer bathymetry of the Gulf of Lions [*Berné et al.*, 2004]. We use a partial cell parameterization, i.e., the bottom layer thickness is varying to fit the real bathymetry.

[9] The values of the first Rossby radius of deformation in the Mediterranean Sea, calculated with the 1998 state of the MEDATLAS-II database [*MEDAR/MEDATLAS Group*, 2002] and with the bathymetry of MED12, are shown in Figure 1b. It gives a precise description of the spatial variations of this radius in the Mediterranean Sea. Dividing the horizontal grid cell size of MED12 by this radius (Figure 1c) and taking that a model is eddy-resolving where this ratio is above 1, we consider that MED12 is eddy-resolving only in the open-sea areas, which nevertheless represent the main part of the Mediterranean Sea.

2.2. Physics Parameterizations

[10] A time step of 12 minutes is used. The horizontal eddy diffusivity coefficient is set to 60 m^2.s^{-1} for the tracers (temperature, salinity) using a Laplacian operator (the diffusion is applied along iso-neutral surfaces for the tracers) and the horizontal viscosity coefficient is set to -1.25×10^{10} m^4.s^{-2} for the dynamics (velocity) using of a biharmonic operator. The TVD (Total Variance Dissipation) scheme is used for the tracer advection and the EEN (Energy and ENstrophy conservative) scheme is used for the momentum advection [*Arakawa and Lamb*, 1981; *Barnier et al.*, 2006]. A 1.5 turbulent closure scheme is used for the vertical eddy diffusivity [*Blanke and Delecluse*, 1993], with an enhancement of the vertical diffusivity coefficient up to 10 m^2.s^{-1} in case of unstable stratification. The solar radiation can penetrate into the ocean surface layers [*Bozec et al.*, 2008]. A no-slip lateral boundary condition is

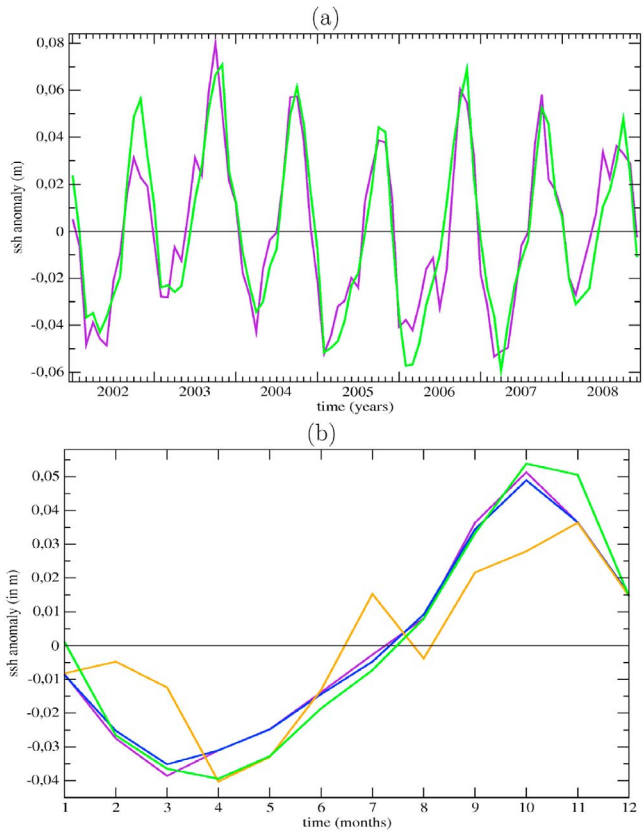

Figure 2. Monthly Sea Surface Height anomaly (m) averaged over the area [11–7.5°W, 32–39°N] (ABZ in Figure 1a) calculated by substracting the 2002–2008 SSH mean for each data set. (a) For the period 2002–2008, interannual (84 monthly) values of (purple) GLORYS-1 are compared to (green) AVISO. (b) In average for the period 2002–2008, monthly climatological values are compared between data sets: (blue) MED12-ARPERA, (purple) GLORYS-1 and (green) AVISO. In orange is added the climatological anomalies of SSH which are used in MED12-ARPERA during the 1998–2001 period.

used. The evolution of the sea surface is parameterized by a filtered free-surface [*Roullet and Madec*, 2000]. The conservation of the model volume is assumed (see section 2.4). The Sea Surface Height (SSH) is a prognostic variable.

[11] The parameterization of the bottom friction $\vec{F}$ is defined as follows in NEMO:

$$\vec{F} = C_D \sqrt{U_H^2 + V_H^2 + E}\ \overrightarrow{U_H}$$

with C_D the bottom drag coefficient, U_H and V_H respectively the zonal and meridian velocities of the bottom layer, $\overrightarrow{U_H}$ the horizontal bottom speed vector and E the bottom turbulent kinetic energy background. In the simulation MED12-ARPERA, E is a 2D field (Figure 1a), corresponding to the mean tidal energy computed from a tidal model [*Lyard et al.*, 2006]. The mean tidal energy is the highest in the Strait of Gibraltar (maximum value over 10000 $cm^2.s^{-2}$) and has significant values mainly in the Channel of Sicily, in the Gulf of Gabes and in the northern Adriatic Sea.

[12] The increase of the bottom friction value in some areas through the values of the mean tidal energy at the bottom is a first step to improve the parameterization of the strait exchanges constrained by the tides. Because our parameterization does not changed the vertical eddy diffusivity, its influence is relatively small compared to other studies using additional information from a tidal model, as obtained by *Koch-Larrouy et al.* [2007]. In particular, the inflowing and outflowing water volume transports through the Strait of Gibraltar are not significantly changed with the new parameterization (differences smaller than 1.5%), compared to the increase of 30% that can be obtained by using a coupling with a tidal model [*Sannino et al.*, 2004].

2.3. Initial Conditions in the Mediterranean Domain

[13] For the Mediterranean Sea, the initial conditions are provided by the monthly mean potential temperature and salinity 3D fields from the MEDATLAS-II climatology [*MEDAR/MEDATLAS Group*, 2002] corresponding to October. These fields are ponderated by a low-pass filtering with a time-window of three years using the MEDATLAS data covering the 1997–1999 period. The simulation then starts with initial conditions close to the Mediterranean Sea state of October 1998 and an ocean at rest.

2.4. Atlantic Boundary Conditions

[14] The exchanges with the Atlantic ocean are performed through a buffer zone. From 11°W to 7.5°W (ABZ in Figure 1a), 3D temperature and salinity of MED12 are relaxed toward the θ-S climatological fields of *Levitus et al.* [2005]. The restoring term is weak west of Cadiz and Gibraltar area (τ = 90 days at 7.5°W) and increases westward (τ = 2 days at 11°W).

[15] The Mediterranean Sea is known as a basin of net evaporation compensated by the Atlantic inflow. According to the NEMO filtered free sea surface parameterization, only the volume of the first level of the model can change but the total volume of the model is not conserved, which requires thus a parameterization to do so. In previous Mediterranean configurations [e.g., *Tonani et al.*, 2008; *Beuvier et al.*, 2010], at each time step, the water volume corresponding to the net evaporation averaged over the Mediterranean Sea (east of Gibraltar) was redistributed in the Atlantic area between 11°W and 7.5°W, as an input of precipitation. In reality, the water evaporated over the Mediterranean Sea does not go back instantaneously in the ocean, and moreover it does not go all in the near Atlantic ocean. Thus, the seasonal cycle of the near Atlantic sea level in simulations with a water volume transfer is the seasonal cycle of the Mediterranean freshwater budget, which has no physical sense.

[16] In MED12-ARPERA simulation, a new parameterization is implemented. The model volume is conserved through a damping of the SSH between 11°W and 7.5°W in the Atlantic buffer zone, toward a prescribed SSH. By doing such a SSH restoring, we try to apply there the seasonal cycle of the water mass in this area, this signal containing the effect of the steric and mass variations at global scales. We apply a very strong restoring, since its time scale is set to 2 seconds. The prescribed SSH was built by adding the mean SSH spatial pattern of a previous companion simulation with monthly SSH anomalies over the Atlantic buffer zone. For the period 2002–2008 (Figure 2a), the

anomalies are taken from GLORYS-1 [*Ferry et al.*, 2010], a reanalysis of the global ocean circulation at a 1/4° horizontal resolution available for this period. For the period 1998–2001, the anomalies are taken from the SSH monthly cycle of the previous companion simulation with a time shift of 5 months in the seasonal cycle to follow the cycle of GLORYS-1 in the near Atlantic domain (Figure 2b). We expect from this SSH restoring in the Atlantic buffer zone to constrain the horizontal pressure gradients at the entrance of the Strait of Gibraltar.

[17] GLORYS-1 anomalies in the Atlantic buffer zone (11°W–7.5°W) have an amplitude of about 14 cm, in agreement with AVISO products (Figure 2a), which were assimilated in the GLORYS-1 reanalysis. The AVISO products used here and in next sections are the weekly Maps of Absolute Dynamic Topography (MADT), equivalent to the SSH from an oceanic model; these MADTs are built by adding weekly satellite Sea Level Anomalies, SLA [*Pujol and Larnicol*, 2005; *Pascual et al.*, 2007], to the reference Mean Dynamic Topography MDT-RioMed2007 [*Rio et al.*, 2007]. AVISO data are produced by Ssalto/Duacs with support from CNES; these data are produced in delayed time, up-to-date and merged modes. During the 2002–2008 period, the correlation between these two times-series (84 monthly values) is 0.94. The amplitude of the interannual variations are of the order of 2 to 4 cm in both products.

2.5. River Runoff and Black Sea Inputs

[18] River inputs are introduced as surface freshwater gain at the river mouths. We use the climatological average of the interannual data set of *Ludwig et al.* [2009] to compute monthly runoff values, split in two parts. First, for the 33 main Mediterranean rivers listed in the RivDis database [*Vörösmarty et al.*, 1996], we directly take the values of the database. Second, the values of the inputs of the other rivers are gathered and averaged in each Mediterranean subbasin (as defined in *Ludwig et al.* [2009]) and put as a coastal runoff in each MED12 coastal grid point of these subbasins. These two types of river inputs contribute for the annual surface freshwater budget of the Mediterranean Sea to +0.09 $m.yr^{-1}$ for the 33 main rivers and to +0.05 $m.yr^{-1}$ for the others, i.e., +0.14 $m.yr^{-1}$ in total, which is in good agreement with the +0.14 $m.yr^{-1}$ estimate of *Boukthir and Barnier* [2000] and higher than the +0.10 $m.yr^{-1}$ estimate of *Mariotti et al.* [2002].

[19] The Black Sea is not included in MED12 but is one of the major freshwater sources of the Mediterranean Sea. The exchanges between the Black Sea and the Aegean Sea consist of a two-layer flow across the Marmara Sea and the Dardanelles Strait. We assume that this flow can be approximated by a freshwater flux diluting the salinity of the mouth grid point. Thus, in the model, the Black Sea is considered as a river for the Aegean Sea, as done in *Beuvier et al.* [2010]. We use the climatological average of the interannual data set of *Stanev and Peneva* [2002] to compute monthly values of the Black Sea net water inflow. The annual average of this input corresponds for the surface freshwater budget of the Mediterranean Sea to +0.10 $m.yr^{-1}$.

[20] The total freshwater input from river and Black Sea runoff amounts thus in our configuration to +0.24 $m.yr^{-1}$.

2.6. Atmospheric Forcing

[21] The atmospheric forcing is ARPERA, obtained by performing a dynamical downscaling of ECMWF products above the European-Mediterranean region [*Herrmann and Somot*, 2008]. The downscaling method used here is a spectral nudging: it uses the atmospheric model ARPEGE-Climate [*Déqué and Piedelievre*, 1995] (grid stretched over the Mediterranean Sea, resolution of 50 km), in which large scales (above 250 km) are spectrally driven by ECMWF fields and small scales (below 250 km) can develop freely. This data set has a realistic synoptic chronology thanks to ECMWF fields and high-resolution structures thanks to the atmospheric resolution of ARPEGE-Climate. The simulated period lasts from the 1st October 1998 to the 31st December 2008. For the period 1998–2001, the driven fields come from the ERA40 reanalysis [*Simmons and Gibson*, 2000]. From 2002 to 2008, fields of the ECMWF analyses are used, their resolution (0.5°∼55 km) being downgraded to the ERA40 resolution (1.125°∼125 km) to insure consistency between the 1998–2001 and 2002–2008 periods. ARPERA follows the real atmospheric chronology and is relevant to model realistically deep convection [*Beuvier et al.*, 2010; *Herrmann et al.*, 2010]. MED12 is forced by ARPERA daily fields of the momentum, freshwater and heat fluxes.

[22] For the surface temperature condition, a relaxation term toward ERA40 Sea Surface Temperature (SST) is applied for the heat flux. This term actually plays the role of a first-order coupling between the SST of the ocean model and the atmospheric heat flux [*Barnier et al.*, 1995], ensuring the consistency between those two terms. The value of the relaxation coefficient is spatially constant and taken equal to -40 $W.m^{-2}.K^{-1}$, following [*CLIPPER Project Team*, 1999]. It is equivalent to a 1.2-day restoring time scale for a surface layer of 1 m thickness.

[23] For the salinity surface boundary condition, no salinity damping is applied. Following [*Beuvier et al.*, 2010], we add to the surface freshwater flux (E−P−R) a correction term, spatially constant, with a monthly cycle and equivalent in annual average to -0.0083 $mm.d^{-1}$ (-0.003 $m.yr^{-1}$), which is neglectable with respect to the total freshwater budget. These monthly values have been computed by averaging the Sea Surface Salinity (SSS) relaxation term through a previous companion simulation with MED12 and the same atmospheric forcing. The surface freshwater budget is thus balanced without altering the spatial and temporal variations of the freshwater flux and so of the SSS. This correction term is added to the water fluxes coming from the atmospheric fields and from the rivers and Black Sea runoff. We note that the total freshwater loss (P+R−E+correction = -0.53 $m.yr^{-1}$ for the 2002–2008 period over the Mediterranean Sea) is in the range of observations and other modeling studies [*Sanchez-Gomez et al.*, 2011].

3. Validation of the Circulation in the Western Mediterranean

[24] In this section, we focus on the Western Mediterranean and on the winter 2005. After a validation of the mean and interannual behavior of the simulation, we describe the general features of temperature, salinity, and the deep convection in the Gulf of Lions, in particular in winter 2005.

Table 1. 10-Year Averages and Standard Deviations of the Inflowing, Outflowing and Net Fluxes Toward the Mediterranean Sea Through the Strait of Gibraltar[a]

Water Flux (Sv)	Heat Flux ($W.m^{-2}$)	Salt Flux (10^{-3} $psu.yr^{-1}$)
	Inflow	
$+0.73 \pm 0.04$	$+20.62 \pm 1.05$	$+218 \pm 11$
	Outflow	
-0.69 ± 0.04	-14.51 ± 0.74	-217 ± 11
	Net	
$+0.045 \pm 0.006$	$+6.11 \pm 0.33$	$+1.8 \pm 1.6$

[a]Water flux is in Sv, heat flux is in $W.m^{-2}$ and salt flux is in 10^{-3} $psu.yr^{-1}$.

3.1. Exchanges Through the Strait of Gibraltar

[25] The 10-year averages and standard deviations of the in, out and net flows of water, heat and salt in the simulation are given in Table 1. The values for the mean water fluxes, +0.73 Sv, −0.69 Sv and +0.045 Sv respectively for the in, out and net flows, are in the lower part of the range given in the literature: between +0.72 and +1.01 Sv for the inflow, between −0.68 and −0.97 Sv for the outflow and between +0.04 and +0.13 Sv for the net flow [*Bryden and Kinder*, 1991; *Bryden et al.*, 1994; *Tsimplis and Bryden*, 2000; *Candela*, 2001; *Baschek et al.*, 2001; *Lafuente et al.*, 2002]. The interannual variations for such a short period, ±0.006 Sv in the simulation, are in agreement with *Soto-Navarro et al.* [2010], who estimate the water outflow during the 2004–2009 period with currentmeter observations. They give values of +0.81 ± 0.06 Sv for the water inflow, −0.78 ± 0.05 Sv for the water outflow and +0.038 ± 0.007 Sv for the net water flow. For the mean net heat flux, the value of +6.1 $W.m^{-2}$ in the simulation is in the range of the estimations of *Béthoux* [1979] ([4; 10] $W.m^{-2}$) and of *Macdonald et al.* [1994] ([3.9; 6.5] $W.m^{-2}$). For the net salt flux, the value corresponds to the trend of the Mediterranean salt content in the simulation, and in thus quite small ($+1.810^{-2}$ psu in 10 years).

3.2. Modeling the SSH Variability

[26] To estimate the impact of the SSH restoring in the Atlantic area applied in MED12-ARPERA, we first look at the SSH values for the simulation and at AVISO data, in averaged over the Mediterranean Sea (Figure 3). We also use the derived geostrophic currents. As the global steric signal is introduced in the model via the SSH damping in the Atlantic buffer zone to the total SSH anomalies from a global reanalysis, we do not add in our comparison the local steric effect in the Mediterranean SSH of the simulation. The peak-to-peak amplitude of the SSH variations in MED12-ARPERA (26 cm) are of the order of those of AVISO. The correlation between AVISO and MED12-ARPERA time series (computed with the 536 de-trended weekly values) is 0.83. This agreement confirms the better physical consistency of a SSH damping in the Atlantic domain than the one of the water redistribution.

[27] Figure 4 then illustrates the ability of MED12-ARPERA to reproduce the time-space variability of the SSH and of the surface currents in the Western Mediterranean Sea, in average over the 2004–2008 period. First, comparing Figures 4a and 4c shows that MED12-ARPERA reproduces the mesoscale variability in the Alboran and Algerian subbasins, with values of SSH RMS (Root Mean Square) corresponding to those from AVISO (between 10 and 14 cm). In the Tyrrhenian subbasin, the simulation slightly underestimates the SSH RMS but reproduces an area with high variability east off the coasts of Sardinia, near the Bonifacio eddy [*Millot and Taupier-Letage*, 2005]. In the northwestern Mediterranean, the variability of the sea surface height is still lower in the simulation than in AVISO. MED12-ARPERA nevertheless reproduces higher SSH RMS

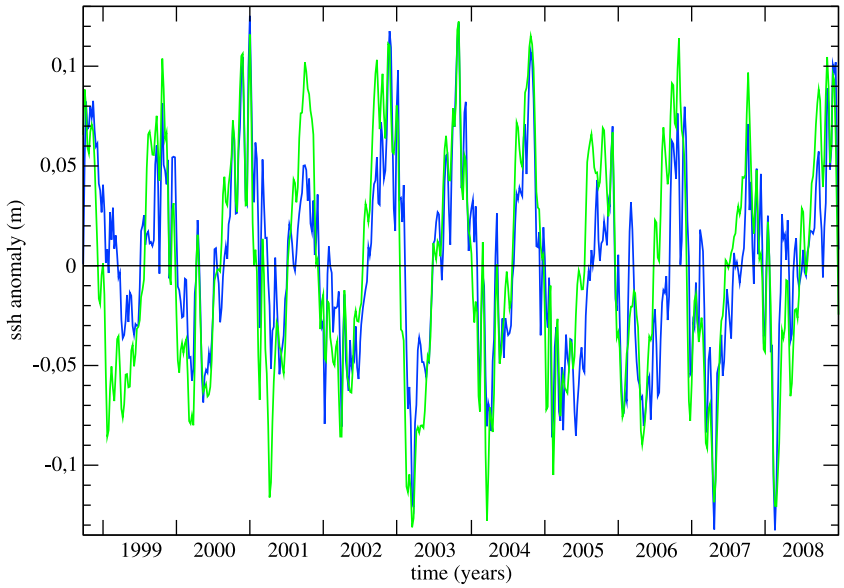

Figure 3. Weekly SSH anomalies (m) averaged over the Mediterranean Sea during the 10-year studied period for (blue) MED12-ARPERA and (green) AVISO. For each data set, anomalies are computed around the average from October 1998 to December 2008.

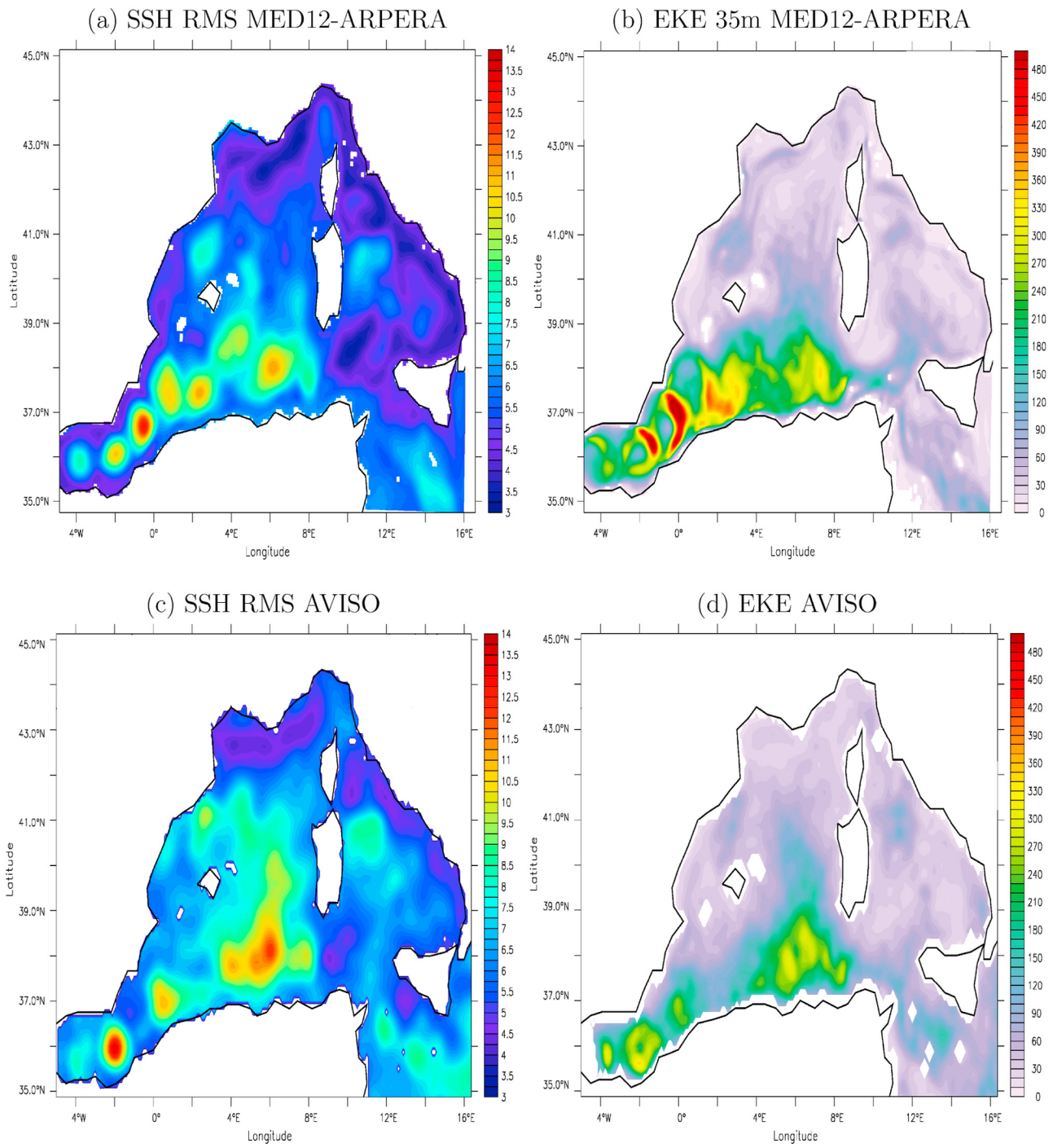

Figure 4. 2004–2008 averages, over the Western Mediterranean, of the RMS of the SSH (SSH Root Mean Square in cm) for (a) MED12-ARPERA and (c) AVISO, and the EKE (Eddy Kinetic Energy in $cm^2.s^{-2}$) for (b) MED12-ARPERA and (d) AVISO. To be consistent with the AVISO geostrophic currents used to calculate the EKE, we took the 35m-depth currents of MED12-ARPERA, i.e., approximately under the mean Ekman layer.

in the Catalan subbasin, as in the observations. Second, we compare the EKE (Eddy Kinetic Energy) of the geostrophic currents from AVISO to the EKE of the MED12-AREPRA currents under the Ekman layer (we take these currents at about 35 m depth). In the Algerian Current area, MED12-ARPERA shows higher eddy circulation, up to an EKE of 500 $cm^2.s^{-2}$, than in AVISO, which gives EKE up to 300 $cm^2.s^{-2}$, and 350 $cm^2.s^{-2}$ in the Eastern Alboran Eddy (as named by *Vargas-Yáñez et al.* [2002]). Elsewhere in the Western Mediterranean, the mean EKE value in the simulation is lower than in AVISO but shows more spatial variability, due to the higher space-time resolution of MED12-ARPERA (6–8 km for daily outputs) if compared to the resolution of AVISO products (about 12 km for

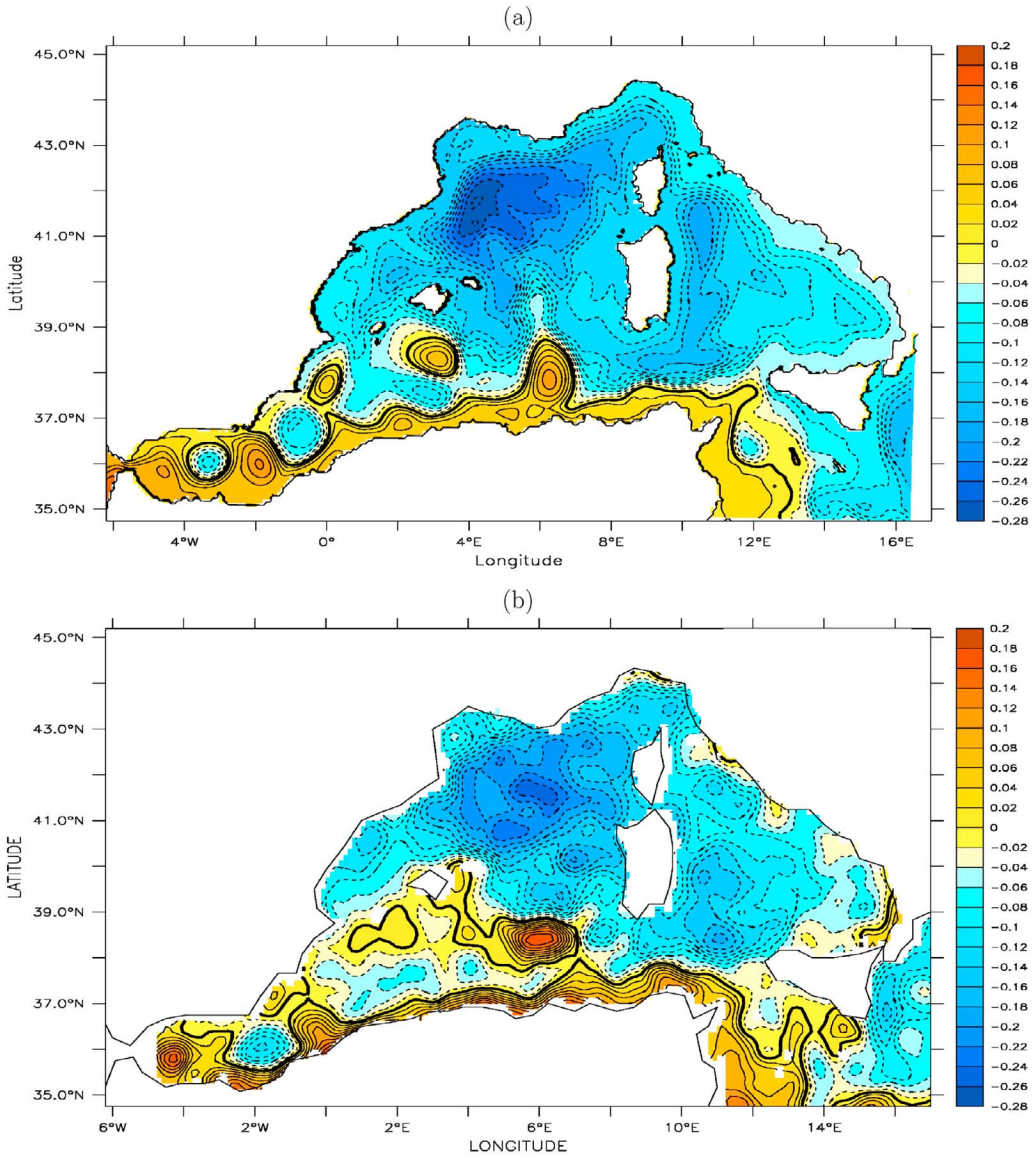

Figure 5. Monthly mean of the SSH (m) over the Western Mediterranean, for February 2005, (a) for simulation MED12-ARPERA and (b) for AVISO. Contours are every 0.02 m, with dashed lines for negative values (cyclonic) and full lines for positive values (anticyclonic).

weekly data). Moreover, the correlation scale applied to the objective analysis in AVISO products is of the order of 100 km, which means that the typical size of structures resolved by this product is of that order [*Pujol and Larnicol*, 2005].

[28] In the following sections, we will focus on the dense water formation in the Gulf of Lions during winter 2005. We thus compare the surface circulation in February 2005 in the western Mediterranean for MED12-ARPERA and AVISO (Figure 5). Some patterns of the large scale circulation are relatively well reproduced for this month. The surface circulation is cyclonic with the AW which enters the Mediterranean Sea through the Strait of Gibraltar. The two anti-cyclonic gyres in the Alboran Sea are present, even if their locations differ a little between the model and the observations. Then the shallow Algerian Current flows eastward along the African coast and anticyclonic eddies more or less detached from the coast are depicted. Anticyclonic areas near 2°E and 6°E at around 38°N are in agreement in both products. The Algerian Current crosses then the Channel of Sardinia and splits in several branches at the level of the Channel of Sicily. One branch enters the Tyrrhenian subbasin and circulates along the Italian coast before crossing the Strait of Corsica, generating there part of the Northern Current. This current then partly retroflects near 4°E to form the cyclonic gyre of the Gulf of Lions, well marked in February 2005. It is centered near 42°N−4°E in the model and near 41.5°N−6°E in the observations. The SSH in the gyre of the Gulf of Lions is of the order and lower than −20 cm for both products in the area [40−43°N; 3−8°E]. A part of the Northern Current flows southwestward off the Balearic islands. The differences between the simulation and the altimetric data are mainly seen at mesoscale, the large scale being in agreement between both products.

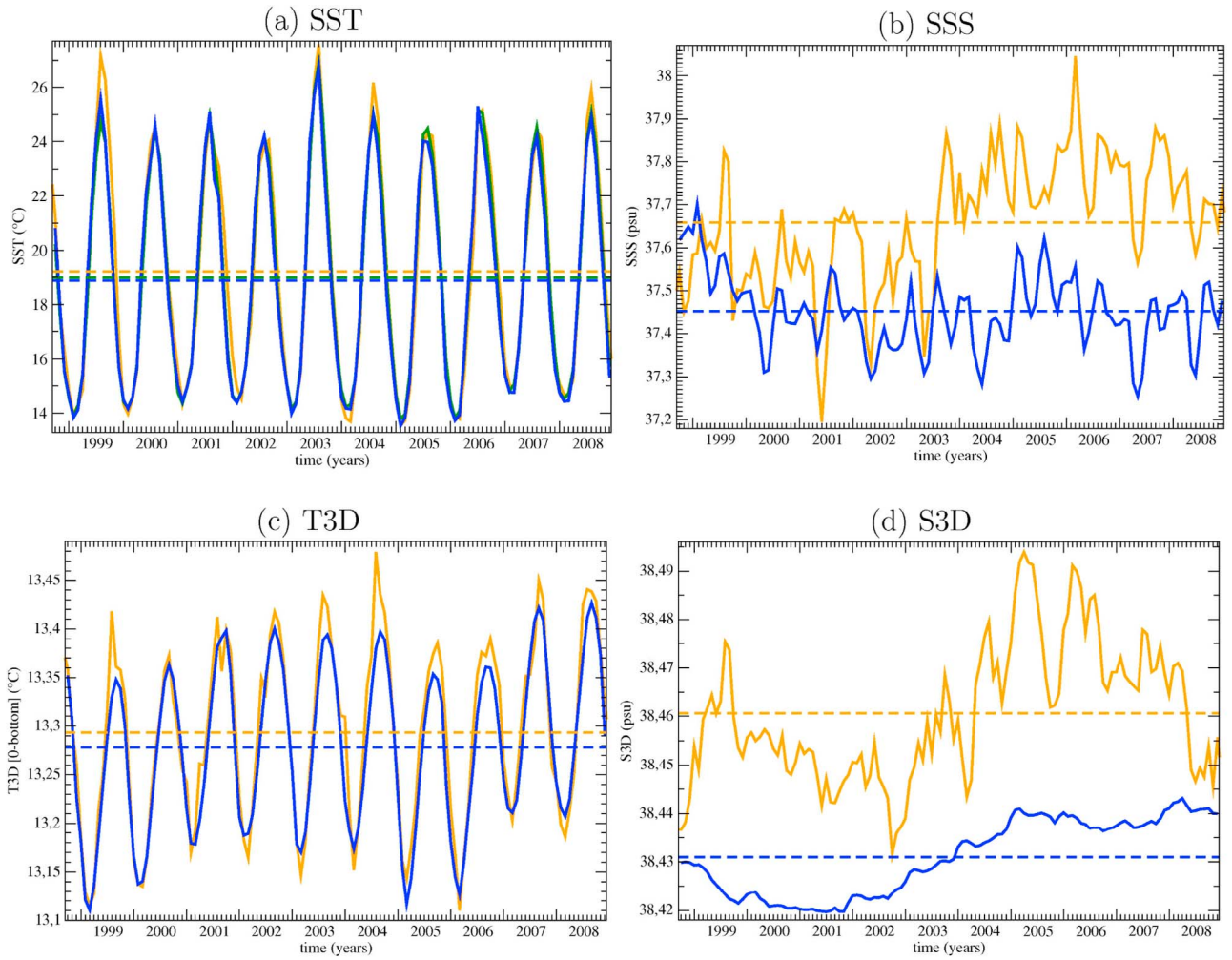

Figure 6. Monthly time series, from October 1998 to December 2008, of the Western Mediterranean averages of (a) the sea surface temperature (SST in °C), (b) the sea surface salinity (SSS in psu), (c) the total heat content (shown as a mean potential temperature T3D in °C) and (d) the total salt content (shown as a mean salinity S3D in psu). MED12-ARPERA is in blue, the EN3 data set [*Ingleby and Huddleston*, 2007] is in orange and the ERA40/ECMWF SST [*Reynolds et al.*, 2002] is in green. Full lines indicate the monthly values, dashed lines correspond to the averages over the period October 1998–December 2008.

These mesoscale differences can be explained by the fact that the simulation is a free run, it is thus very difficult to reproduce the exact location and intensity of mesoscale eddies without data assimilation.

3.3. Interannual Thermohaline Characteristics in the Western Mediterranean

[29] To study the representativity of the interannual variability in the simulation in the Western Mediterranean, we analyzed the evolution of the SST, SSS, heat and salt contents (Figure 6), averaged over the Western Mediterranean, i.e., between the Strait of Gibraltar and the Channel of Sicily.

[30] For the SST (Figure 6a), we compare the monthly means of MED12-ARPERA in blue, of the EN3 data set [*Ingleby and Huddleston*, 2007] in orange and of the ERA40/ECMWF SST [*Reynolds et al.*, 2002] in green. In average over the simulated period, the mean Western Mediterranean SST is 18.88°C for MED12-ARPERA, 18.99°C for Reynolds and 19.22°C for EN3. The monthly variability is very well reproduced in the simulation, thanks to the retroaction term in the forcing heat flux. The interannual variations of the winter minima and summer maxima are also well simulated, except for warm summers in 1999, 2003, 2004 and 2008, during which MED12-ARPERA SST is slightly lower than EN3 SST.

[31] For the SSS (Figure 6b), we compare the averages over the Western Mediterranean for MED12-ARPERA (blue) and EN3 (orange). In average over the simulated period, the mean Western Mediterranean SSS is 37.45 psu for MED12-ARPERA and 37.66 psu for EN3. We remind here that there is no sea surface salinity restoring in the simulation. The sharp SSS increase (jump) in EN3, which can be attributed to the heat wave of summer 2003, is not reproduced in the model and then can explain an important part of the total 10-year bias of MED12-ARPERA SSS in the Western Mediterranean.

[32] For the Western Mediterranean total heat content (given as a mean potential temperature T3D in Figure 6c),

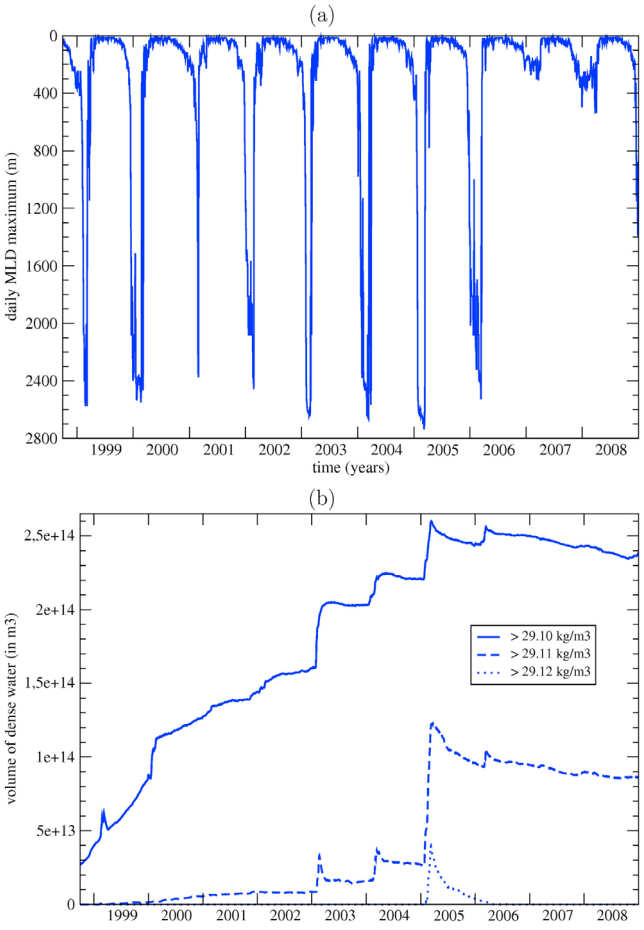

Figure 7. Daily values, from the 1st October 1998 to the 1st December 2008, of (a) the maximum of the turbocline depth (m) in the northwestern Mediterranean (cf. Figure 1a), and (b) the volume (in m^3) of dense waters in the northwestern Mediterranean for three thresholds: denser than 29.10 (solid lines), 29.11 (dashed lines) and 29.12 $kg.m^{-3}$ (dotted lines).

the simulation has a slight cold bias, the mean value over the simulated period being 13.28°C for MED12-ARPERA (blue line) and 13.29°C for EN3 (orange line). The seasonal and interannual variations are well reproduced in the simulation, with a slightly lower amplitude of the monthly cycle than in EN3 (winters less cold and summers less warm in the simulation). In both the simulation and the observed data set, very cold winters like those of 1999, 2005 and 2006 are identified by the lowest potential temperature values (below 13.15°C in winter), while other years can be considered as relative warm winters, especially 2007 and 2008, for which the minimum value is higher than 13.2°C in winter. This alternation of cold and warm winters will be linked further to the occurrence or not of dense water formation in the Gulf of Lions.

[33] For the Western Mediterranean total salt content (given as a mean salinity S3D in Figure 6d), the simulation has a fresh bias, the mean value over the simulated period being 38.43 psu for MED12-ARPERA (blue line) and 38.46 psu for EN3 (orange line). The simulation shows alternative periods of salinity decrease or increases before and after end-2001, but these variations have a far higher amplitude in EN3. The difference in the amplitude of the monthly variations of S3D between MED12-ARPERA and EN3 can be due to shortcomings in the model, but one has to remind that issues due to undersampling may artificially increase the monthly variations in data sets coming from in-situ observations, especially for salinity.

[34] Deep convection occurs in the Gulf of Lions during the 10-year period as deduced from the time series of the daily spatial maximum reached by the convection in the northwestern Mediterranean (Figure 7a). In particular, the convection reaches depths higher than 2000 m depth for events longer than two months in 2000, 2004 and 2006, and longer than one month and a half from end January to early March 2005. We also note that no deep convection occurs in 2007 and 2008 in the simulation. These time-series are in agreement with another modeling work obtained after a 15-year spin-up [*Béranger et al.*, 2009], showing thus some skills of such short simulations to represent the interannual variability of the general circulation. Looking at the evolution of the volume of dense waters in the northwestern Mediterranean (Figure 7b), we identify the WMDW with the usual density threshold of 29.10 $kg.m^{-3}$, but we also use denser thresholds to highlight the exceptionality of winter 2005 and to better identify the new WMDW. Despite the first two years of spin-up, we can identify that water denser than 29.10 $kg.m^{-3}$ is formed during winters 1999, 2000, 2003, 2004, 2005 and 2006. Water denser than 29.11 $kg.m^{-3}$ is formed during winter 2005 in larger quantities compared to winters 2003, 2004 and 2006. Water denser than 29.12 $kg.m^{-3}$ is only formed, in sizeable amount, during winter 2005. And in early March 2005, water denser than 29.13 $kg.m^{-3}$ is formed (see Table 2). Thus, the 29.11 $kg.m^{-3}$ can be used in our simulation to characterize the new WMDW and its formation rate in the simulation MED12-ARPERA.

[35] To compare our results with the 2.4 Sv mean estimate over the two winters 2005 and 2006 of *Schroeder et al.* [2008], derived from the volumetric distribution of the θ-S properties in in-situ observations for the end 2004–end 2006 period, we add in Table 2 the dense water formation rates for winter 2006. With the 29.11 threshold, it gives a mean formation rate over these two winters of 1.73 Sv in the simulation. In comparison, for the single winter 2005, *Béranger et al.* [2009] and *Herrmann et al.* [2010] obtained a formation rate of 1.28 Sv and 1.16 Sv respectively, i.e., 2.5 times lower than in MED12-ARPERA (3.05 Sv).

[36] The exceptional winter convection event in 2005 gives the largest volume of dense water formed compared to the 10-year studied period and to other climatological estimates reported in *Marshall and Schott* [1999]. It is also exceptional in terms of spatial extent of the deep

Table 2. Dense Water Formation Rates (in Sv) in the Gulf of Lions for Winters 2005 and 2006

Class/Winter	2005	2006	Mean
≥29.10 $kg.m^{-3}$	1.26	0.42	0.84
≥29.11 $kg.m^{-3}$	3.05	0.41	1.73
≥29.12 $kg.m^{-3}$	1.26	0.00	0.63
≥29.13 $kg.m^{-3}$	0.28	0	0.14

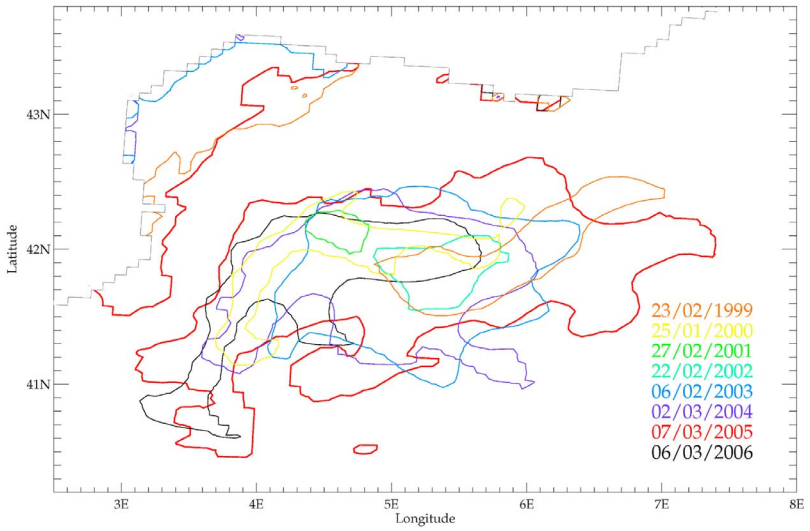

Figure 8. Daily maximal extent of the 29.10 kg.m^{-3} isopycne at the sea surface in the Gulf of Lions, in winter 1999 (orange, 23rd February 1999), 2000 (yellow, 25th January 2000), 2001 (green, 27th February 2001), 2002 (turquoise, 22nd February 2002), 2003 (blue, 06th February 2003), 2004 (purple, 2nd March 2004), 2005 (red, 7th March 2005) and 2006 (black, 6th March 2006), in simulation MED12-ARPERA. In winters 2007 and 2008, the 29.10 kg.m^{-3} isopycne does not reach the sea surface.

convection area. Figure 8 compares the maximal extent of the 29.10 kg.m^{-3} isopycne outcrop at surface for the 10 winters simulated in MED12-ARPERA (in winters 2007 and 2008, this isopycne does not outcrop). Winter 2005 appears to have the widest convection area (about 48000 km^2, see Table 3), in the open sea (from the usual location of 42°N−5°E) as on the shelf of the Gulf of Lions. The deep convection area extends southwestward, downstream of the Northern Current toward the Balearic Islands, but also eastward until 7.5°E. Deep mixed layers have been observed in the eastern Catalan subbasin (4.845°E−39.785°N [*Smith et al.*, 2008]) in early March 2005. The convection area in MED12-ARPERA, as identified in winter 2005 in Figure 8, clearly extends to the eastern part of the Catalan subbasin (Csb in Figure 1a), even if it does not reach the far south position observed. During the other winters in this simulation, the convection does not occur in all these parts of the Gulf of Lions, showing again the exceptional intensity of the convection in winter 2005.

[37] For each winter, the day corresponding to the maximal horizontal extent of the 29.10 kg.m^{-3} isopycne outcrop is also indicated in Figure 8. Winter 2005 has the latest date for this maximal extent, which occurs on the 7th March 2005. It is an other point that underlines the exceptionality of this winter in terms of duration of the severe winter conditions over the Gulf of Lions, well reproduced in the simulation. The occurrence of the maximal extent of the convection area in early March is also consistent with surface chlorophyll concentration observations by MODIS satellite reported in *Herrmann et al.* [2010].

4. Spreading of WMDW After Winter 2005

[38] In this section, we focus on the aim of this study: to characterize, in the simulation, the spreading of the new dense water mass formed in winter 2005, from the convection area in the Gulf of Lions southwards in the Western Mediterranean, and to compare it with in-situ observations made at that time. Then, we adopt successively an Eulerian and a Lagrangian analysis to estimate the transport time and we discuss about the results we obtain.

4.1. θ-S Characteristics of the New WMDW

[39] The temperature and salinity characteristics of waters denser than 29.10 in the Gulf of Lions are shown in Figure 9 for the 1st November 2004, the 7th March 2005, the 1st May 2005 and the 1st November 2005. The densest WMDW at the end of 2004, i.e., before the convection event of 2005, is 29.112 kg.m^{-3} (θ = 12.76–12.78°C, S = 38.440–38.450 psu, Figure 9a); in comparison, the pre-2005 observed thermohaline characteristics of the WMDW are indicated on Figure 9a with the black box, showing that the simulation starts this winter with the good deep water characteristics in

Table 3. Maximal Extent (in km^2) of the Area With Sea Surface Density ≥29.10 kg.m^{-3} in the Northwestern Mediterranean for the 10 Simulated Winters in Simulation MED12-ARPERA[a]

Winter	Maximal Extent (km^2)
1999	16694
2000	6918
2001	1130
2002	3222
2003	20889
2004	19351
2005	47968
2006	17432
2007	0
2008	0
10-year average and standard deviation	13360 ± 14031

[a]See Figure 1a for the boundaries of the northwestern Mediterranean. The average and standard deviations of the 10 yearly maxima are also indicated.

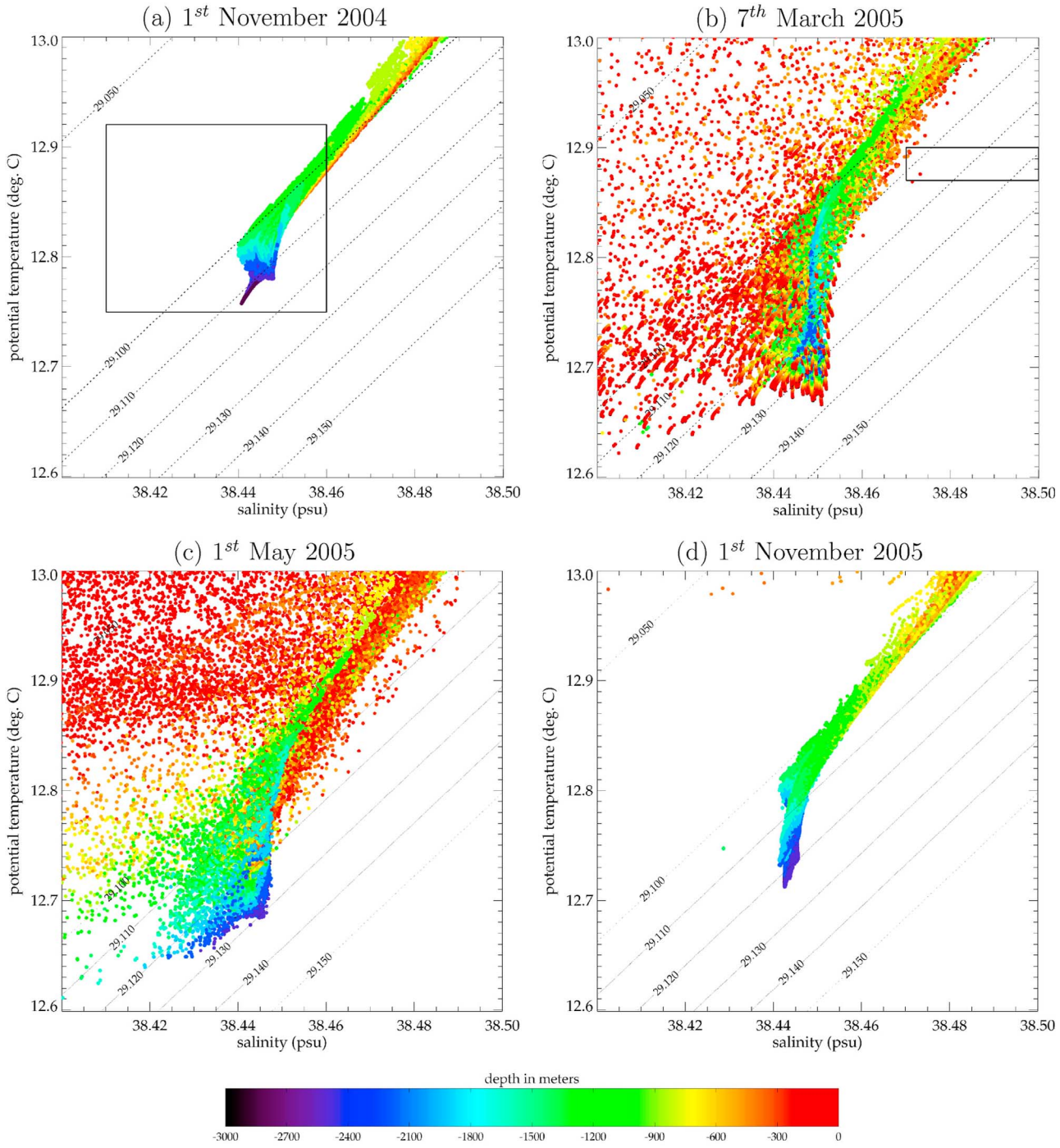

Figure 9. θ-S diagrams in the Gulf of Lions, in simulation MED12-ARPERA, for (a) the 1st November 2004, (b) the 7th March 2005, (c) the 1st May 2005 and (d) the 1st November 2005. The color of the dots indicates the depth in the model. Thin and dashed lines indicate potential density values in kg.m^{-3}. The boxes in Figure 9a and 9b indicate the pre-2005 and 2005 thermohaline characteristics, respectively, of the WMDW found in the literature.

the Gulf of Lions. During the most intense phase of the deep convection event, the 7th March 2005 in the simulation, the new WMDW is characterized by a maximal density of 29.138 kg.m^{-3} (θ = 12.67–12.72°C, S = 38.440–38.453 psu, Figure 9b). Two months later in spring, after the restratification phase, this highest density is still above 29.130 kg.m^{-3} (θ = 12.65–12.71°C, S = 38.435–38.448 psu, Figure 9c) whereas eight months later it has decreased by about 0.01 kg.m^{-3} in the Gulf of Lion toward 29.123 kg.m^{-3} (θ = 12.70–12.75°C, S = 38.442–38.448 psu, Figure 9d). Compared to observations of *López-Jurado et al.* [2005], *Schröder et al.* [2006], *Font et al.*

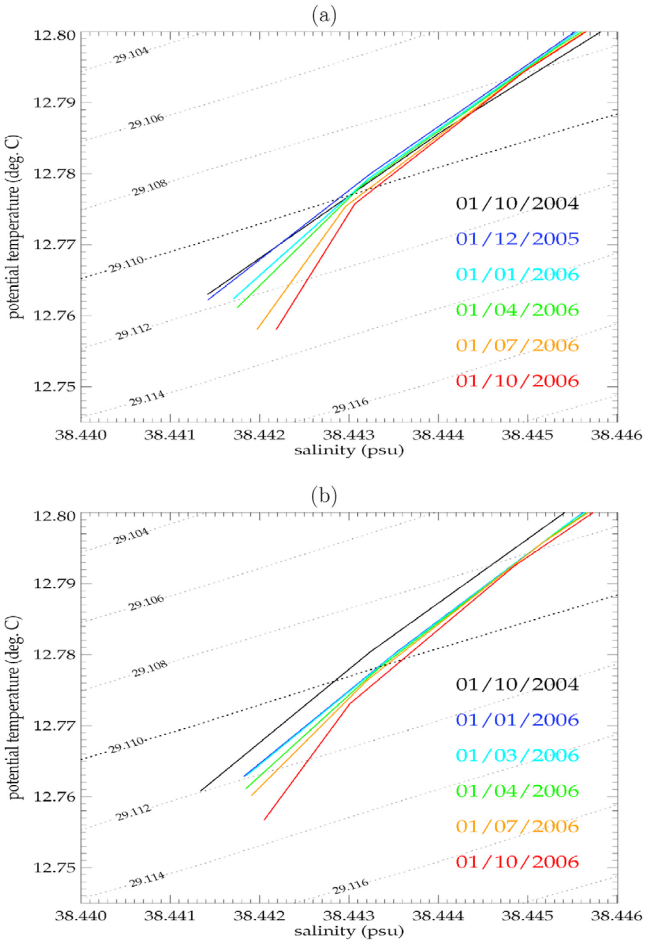

Figure 10. Bottom end of θ-S profiles averaged (a) over the box [8°E;9°E]-[37°N;39°N] (box 1 in Figure 1a, west of the Channel of Sardinia) and (b) over the box [2°E;3°E]-[36.5°N;39°N] (box 2 in Figure 1a, west of the Algerian subbasin), in simulation MED12-ARPERA. Dashed lines indicate potential density values in kg.m^{-3}. The correspondence between dates and colors is indicated within the diagram.

[2007] and *Smith et al.* [2008], who reported θ = 12.87–12.90°C and S = 38.47–38.49 psu (black box in Figure 9b), the thermohaline characteristics of the new WMDW formed in winter 2005 in the model are not warm enough and not salty enough. Obtaining such an agreement is very difficult with a numerical model, mainly because of uncertainties in the initial conditions, the atmospheric fluxes and the physics of the model. Here, it could be related to the presence or not of dense water formed during the Eastern Mediterranean Transient in the early 1990's [*Roether et al.*, 2007] in the simulation or in the initial conditions only. In fact, *Herrmann et al.* [2010] obtained more accurate θ-S characteristics for the new WMDW with the same ARPERA atmospheric forcing but within a 46-year simulation, containing thus a well simulated EMT and not only an EMT hardly present in the initial state of the simulation, as we do. Nevertheless, the density signature is in agreement with observations in our simulation, allowing us to follow the deep water mass propagation in the model.

4.2. θ-S Characteristics in the South of the Western Mediterranean

[40] Following the observations of *Schroeder et al.* [2008], we look at the thermohaline characteristics of waters near the Channel of Sardinia and the Strait of Gibraltar to detect the arrival of the new WMDW at these places. Even if our results are satisfying for the Channel of Sardinia, the model does not succeed in catching such signature at the Strait of Gibraltar. We consider then the θ-S diagram of waters in two boxes (see Figure 1a), box 1 west of the Channel of Sardinia [8°E;9°E]-[37°N;39°N], and box 2 west of the Algerian subbasin [2°E;3°E]-[36.5°N;39°N]. In the two boxes, the last point of the θ-S diagrams corresponds to 2530 m depth.

[41] For the Sardinian area (Figure 10a), there is no change in the deep thermohaline characteristics between the 1st October 2004 (black line) and the 1st December 2005 (dark blue line). A noticeable change starts to appear during December 2005, since the profile of the 1st January 2006 (light blue line) shows waters slightly denser, colder and saltier than the previous one. Then, these changes continue in the same way and for the 1st October 2006 (red line) the deep water has become denser by 0.002 kg.m^{-3} (ρ = 29.113 kg.m^{-3}), colder by 0.005°C (θ = 12.758°C) and saltier by 0.001 psu (S = 38.442 psu) than before. Thus, in the model, it takes about 9 to 10 months (from February-March to December 2005) for the new WMDW to reach the Channel of Sardinia. The signature of this new water mass is relatively weak because the density of old water is initially of 29.111 at this place, which is relatively high but which corresponds to the density of the old WMDW in the Gulf of Lions (as seen in section 4.1). Nevertheless, reminding that it is obtained for very deep water and by averaging over a box of 1° × 2°, this signature is noticeable.

[42] For the Algerian area (Figure 10b), between the 1st October 2004 (black line) and the 1st January 2006 (dark blue line), the slight deep warming and salting associated with a tiny density decrease are certainly caused by mixing or diffusion with water above and not by the advection of a new water mass, since the new WMDW are colder and denser than the old one. Then, the deep thermohaline characteristics of this area remain almost constant until the 1st March 2006 (light blue line). A significant change starts to appear during March 2006, since the profile of the 1st April 2006 (green line) shows waters slightly colder and denser than the previous one. Then, the profile for the 1st October 2006 (red line) is denser, colder and saltier than 9 months before, changes and new characteristics being similar as those of the Sardinian area. Thus, in the model, it takes about 12 to 13 months (from February-March 2005 to March 2006) for the new WMDW to reach the deep area between the Balearic islands and the Algerian coast.

4.3. Transport Estimates

4.3.1. Eulerian Considerations

[43] Using the results of the simulation MED12-ARPERA, we follow the deep spreading of the new WMDW formed in winter 2005. As argued in section 3.3, the core of the new WMDW in the model is identified by the 29.11 kg.m^{-3} threshold. The depth of the σ_0 = 29.11 isopycne (Figure 11) is a first way to follow the propagation of

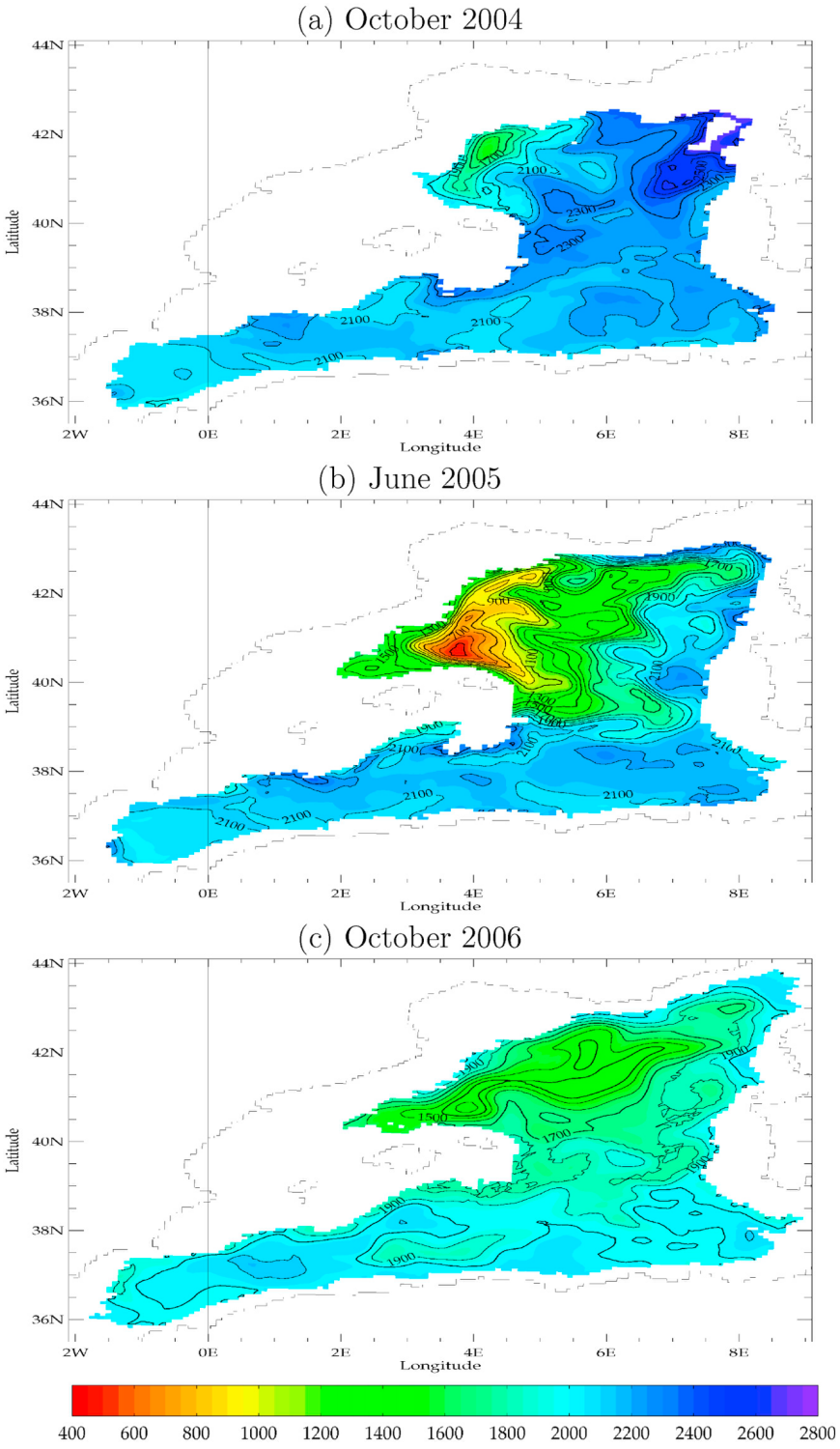

Figure 11. Monthly averages of the depth (in meters, contour lines every 100 m) of the σ_0 = 29.11 isopycnal surface, for (a) October 2004, (b) June 2005 and (c) October 2006.

the new WMDW. To favor the comparison with observations, we choose the same dates as in *Schroeder et al.* [2008]. In October 2004 (Figure 11a), the preconditioning due to the cyclonic gyre in the Gulf of Lions is obvious, inducing a doming of the isopycnal surfaces and thus the 29.11 isopycne depth is less than 1600 m in this area. In the other part of the Algero-Provencal subbasin, the isopycnal surface is deeper than 2100 m, and even deeper than 2500 m near the Ligurian subbasin (Lsb in Figure 1a). There is no water with such a density or denser in the Catalan subbasin (Csb in Figure 1a) and in the center of the Ligurian subbasin. In June 2005 (Figure 11b), i.e., 3 months after the end of the

deep convection event, the core of the recently formed water mass is located between the Gulf of Lions and the Balearic Islands, and the 29.11 isopycne is shallower than 500 m. New WMDW is present in the eastern part of the Catalan subbasin (in consistency with the occurrence of deep convection in this area, as described in Figure 8) and flows along the continental slope off the coast of Minorca Island (easternmost island of the Balearic archipelago). From the convection area, the new WMDW spreads also to the east toward the center of the subbasin. In October 2006 (Figure 11c), the 29.11 isopycne is located at lower depth in the northwestern part of the subbasin, because of the steady cyclonic circulation. But it is obvious that in all the Western Mediterranean, the isopycnal surface has been uplifted, compared with the ocean state two years before. This uplift is of the order of about 200 m in the area between the Algerian coast and the Balearic Islands, with higher differences along the Balearic continental slope. The uplift amounts to 400 m in the center of the cyclonic gyre of the Gulf of Lions (from less than 1600 m in October 2004 to less than 1200 m in October 2006). The uplift is the most substantial in the Ligurian subbasin, in which the depth of the 29.11 isopycne varies from 2700 m in October 2004 to about 1800 m in October 2006. This is in good agreement with *Schroeder et al.* [2008], who evidenced an uplift of the σ_{1000} = 33.477 isopycne of about 100–150 m in the southern part of the subbasin and 200 m in the northern part, up to 1000 m in the Ligurian subbasin.

[44] Figure 12 shows the potential density and the horizontal current at 2225 m depth for different days from mid-June to end-December 2005. In June 2005 (Figure 12a), i.e., 3 months after the end of the deep convection event, the densest waters have started to exit the former convection area (around 42°N−5°E) and flow southwards along the slope of the Balearic Islands between 42°N and 40°N; the potential density is still high (≥29.125 kg.m^{-3}). A cyclone, identified by C1 in Figure 12a, starts to trap dense water and to carry it quicker southwards. The separation of the cyclone from the core of the dense water flow seems to be made easier by a northwestward intrusion of light water, obvious around 41°N−5°E. About one month later in early August 2005 (Figure 12b), the cyclone C1 is well defined, around 39°N−5.5°E, with a density gradient higher than 0.01 kg.m^{-3} between the center and the surrounding of the cyclone. It has an horizontal extent of about 1.5° × 1°, with an elliptic shape. A second cyclone, identified by C2 in Figure 12b, starts to form within the densest part of the water mass (near 40.5°N−4.5°E). At the end of August 2005 (Figure 12c), C1 is now located between 38°N and 39°N, while C2 starts to move southwards, still along the continental slope of the Balearic Islands. At the end of October 2005 (Figure 12d), the signature of C1 is less obvious, while C2 is separating from the flow of the densest water mass. Again, an intrusion of light water occurs simultaneously with the separation of the cyclone C2. In early December 2005 (Figure 12e), C2 can be identified at about 39°N, with an horizontal extent of about 1° × 1° and a more circular shape than C1. A third cyclonic eddy, named C3, starts to appear near 40.5°N−4.5°E. At the end of December 2005 (Figure 12f), C3 crosses the 40°N line and C2 is not identifiable anymore, even if the dense water mass signature which was previously associated with it ($\rho \geq 29.115$ kg.m^{-3}) is still noticeable at 5°E and between 38°N and 39°N. At the end of December 2005, the deep circulation in the Algerian subbasin is more constrained by the cyclonic eastern Algerian gyre (identified by *Testor et al.* [2005]) than for previous dates.

[45] A vertical section through the cyclone C1 at the date of Figure 12b (early August 2005) enables to define the vertical signature of this eddy. Figure 13a shows the meridian speed and the potential density across C1. A maximum meridian speed of 24 cm.s^{-1} is reached at the surface. It is obvious that C1 is barotropic since it has a vertical extent from the bottom to the surface of the sea. It induces a doming of the isopycnal surfaces, particularly noticeable below the stratified summer surface layer. The layer of water denser than 29.11 kg.m^{-3} is about 1500 m thick in the center of the cyclone, with a weak vertical stratification. Inside C1, below 700 m depth, θ ranges between 12.71 and 12.85°C and S ranges between 38.44 and 38.45 psu (Figure 13b). This corresponds well with the values found in the Gulf of Lions during and after the convection event in the simulation. Again, it highlights that the new WMDW in the model is not warm enough and not salty enough compared to in-situ observations made at that time. Around C1, the warm and salty LIW layer is well identifiable, with a core at about 400 m depth ($\theta \geq 13.40$°C, S ≥ 38.55 psu). The vertical doming induced by C1 is also noticeable for the isothermal and isohaline surfaces (Figure 13b).

[46] We have shown with Figure 13 that C1 is a barotropic cyclone. So are C2 and C3 (not shown). Thus, their signature in terms of currents can be seen until the sea surface. The Sea Surface Height (SSH) of the model can be used to follow the paths of these cyclonic eddies (Figure 14). The comparison between the SSH and the Barotropic Stream Function (BSF, Figure 15) allows to distinguish, among the surface eddies identifiable with the SSH, those which are barotropic and which thus carry water throughout the whole water column. Figure 15 shows the same dates as Figures 12 and 14 to easily identify the same cyclones C1, C2 and C3. From June 2005 to December 2005, the cyclonic eddies previously identified have the highest values of BSF in the center of the Algero-Provencal subbasin. About 15 Sv of water over the whole column are carried southwards by C1 in June 2005 (Figure 15a), at most 10 Sv are carried southwards by C2 (Figure 15b) and at most 7 Sv are carried southwards by C3 (Figure 15e). In terms of SSH (Figure 14), the three successive barotropic cyclones have a surface signature and move southwards off the coast of Minorca, from 40°N to 38°N, between 5°E and 6°E. In the model, the southwards propagation of these three successive cyclones lasts more than 6 months, from June 2005 to December 2005.

[47] A comparison with an observed SSH could assess if the eddies identified by the SSH of the model are realistic, and thus if the occurrence of deep barotropic cyclones during summer 2005 is credible. Here again, we use the weekly MADTs of AVISO (Figure 16). In the observations, two cyclones, CA and CB, propagate successively southwards off the coast of Minorca between early-June 2005 (Figure 16a) and early August 2005 (Figure 16e). At the end of August 2005, no cyclonic eddy is noticeable in the area of interest (not shown). They are located around 5°E, whereas in the model C1, C2 and C3 are around 5.5°E. Nevertheless, the

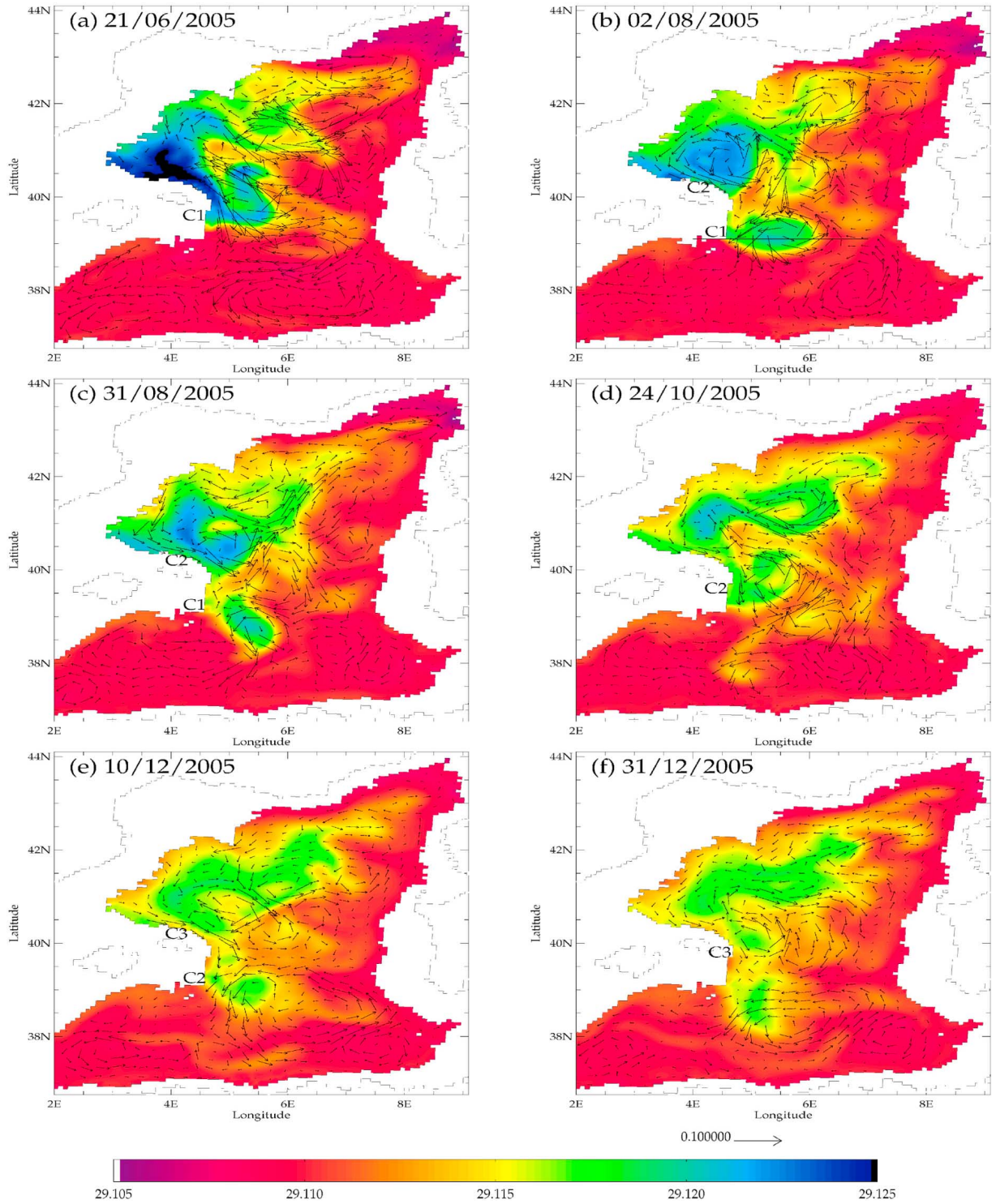

Figure 12. Potential density (colors, in kg.m^{-3}) and currents (arrows, in m.s^{-1}), at 2225 m depth, for (a) the 21st June 2005, (b) the 2nd August 2005, (c) the 31st August 2005, (d) the 24th October 2005, (e) the 10th December 2005 and (f) the 31st December 2005. One vector in three is plotted. C1, C2 and C3 identify the three successive deep cyclones. The section of Figure 13 is drawn on Figure 12b.

occurrence of cyclonic eddies propagating southeastward then southwards near 40°N−5°E is realistic and confirmed by satellite observations. The time transport of these eddies is estimated at about 2 months. It is about 4 months shorter than in the simulation MED12-ARPERA. This slower propagation in the model could be explained by a fewer volume of dense water formed in the model than in reality, which could hinder the spreading of dense water. The vertical resolution of the deep layers in the model could also explain the difficulty of the model to horizontally propagate

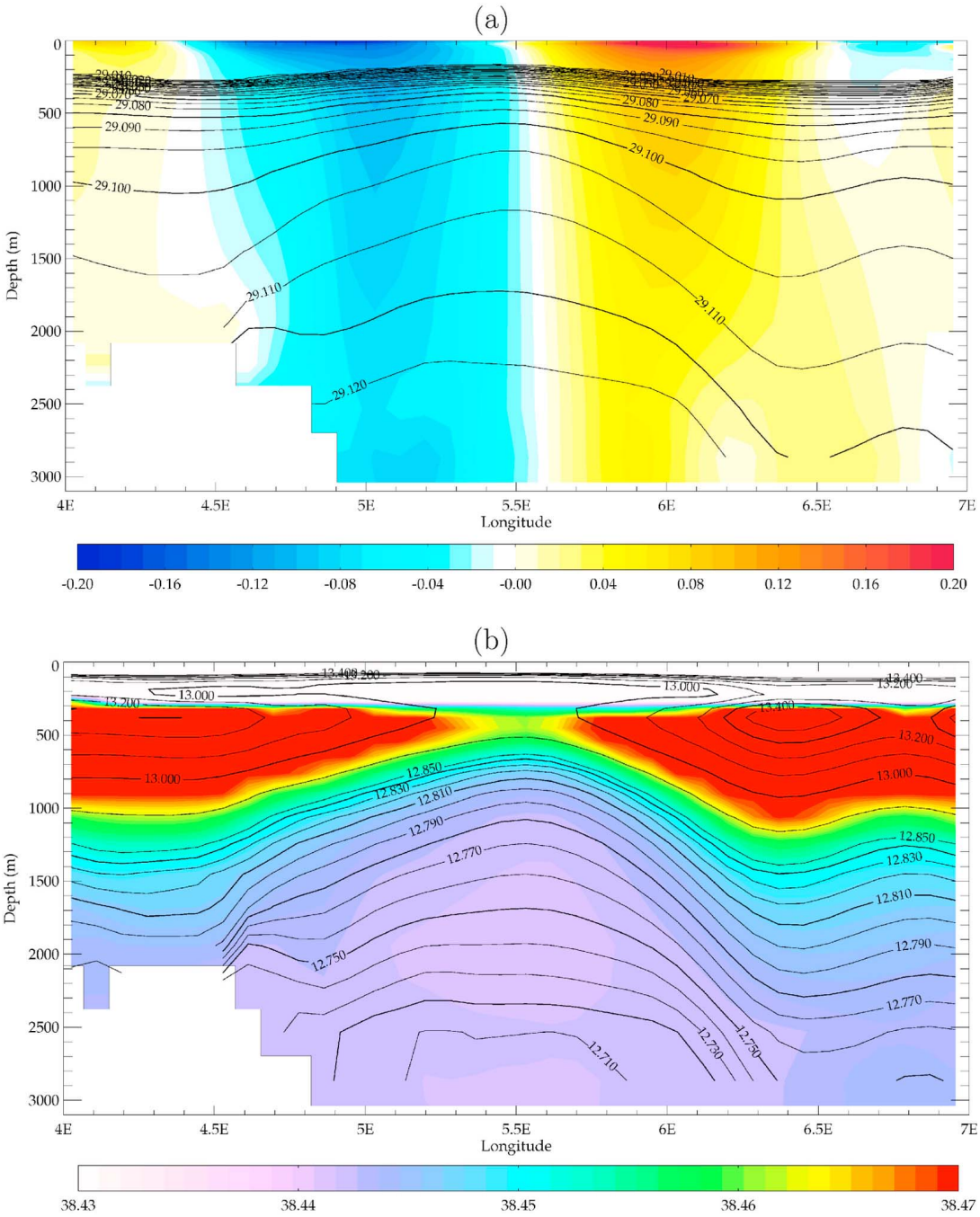

Figure 13. Vertical sections at 39.1°N through cyclone C1, in simulation MED12-ARPERA for the 2nd August 2005. (a) Meridian speed (colors, in $m.s^{-1}$, negative values for southwards current, positive values for northwards current) and potential density (in $kg.m^{-3}$, contour lines from 29.00 $kg.m^{-3}$ every 0.005 $kg.m^{-3}$). (b) Salinity (colors, in psu) and potential temperature (in °C, contour lines every 0.01°C up to 12.85°C, then every 0.1°C from 12.9°C to 13.5°C).

such dense water mass quickly enough. Finally, *Herrmann et al.* [2008] have shown that the horizontal resolution of the model plays also a role, not only on the spatial scale of the processes that can be resolved by an ocean circulation model, but also on the formation of more energetic eddies. Increasing the horizontal resolution would thus certainly lead to a better representation of the advection time of deep water by barotropic eddies.

4.3.2. Lagrangian View

[48] We adopt here a Lagrangian approach to follow the spreading of the new WMDW formed in winter 2005. We use ARIANE [*Blanke and Raynaud*, 1997], a Lagrangian simulator of particles, in an offline configuration with the daily outputs of horizontal and vertical velocities from the simulation MED12-ARPERA. In ARIANE, particles are only advected in 3D, they are not affected by mixing or

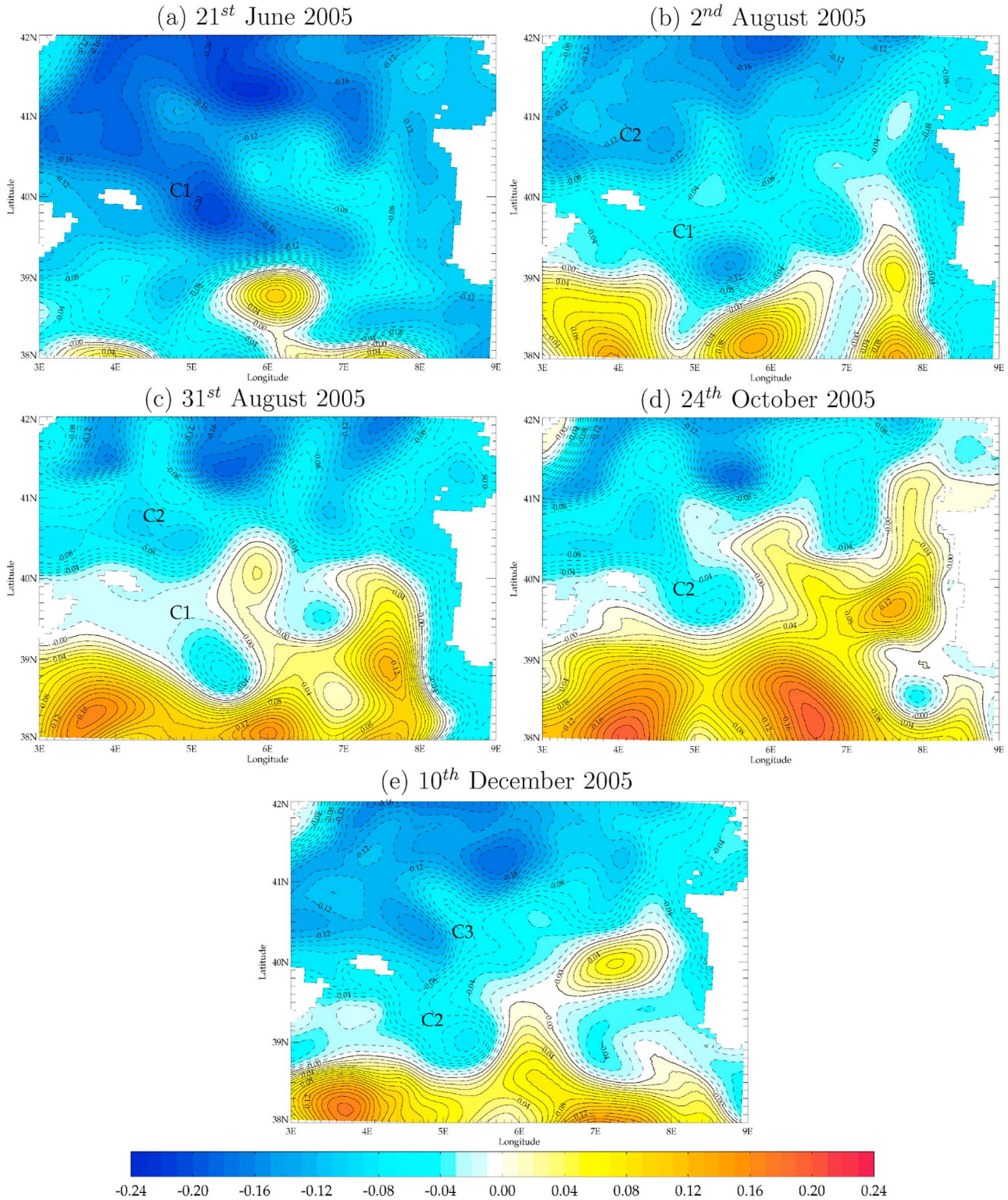

Figure 14. Daily averages of the Sea Surface Height (in meters, contours every 0.01 m), in simulation MED12-ARPERA, in the center of the Western Mediterranean, for (a) the 21st June 2005, (b) the 2nd August 2005, (c) the 31st August 2005, (d) the 24th October 2005 and (e) the 10th December 2005. C1, C2 and C3 identify the three successive deep cyclones.

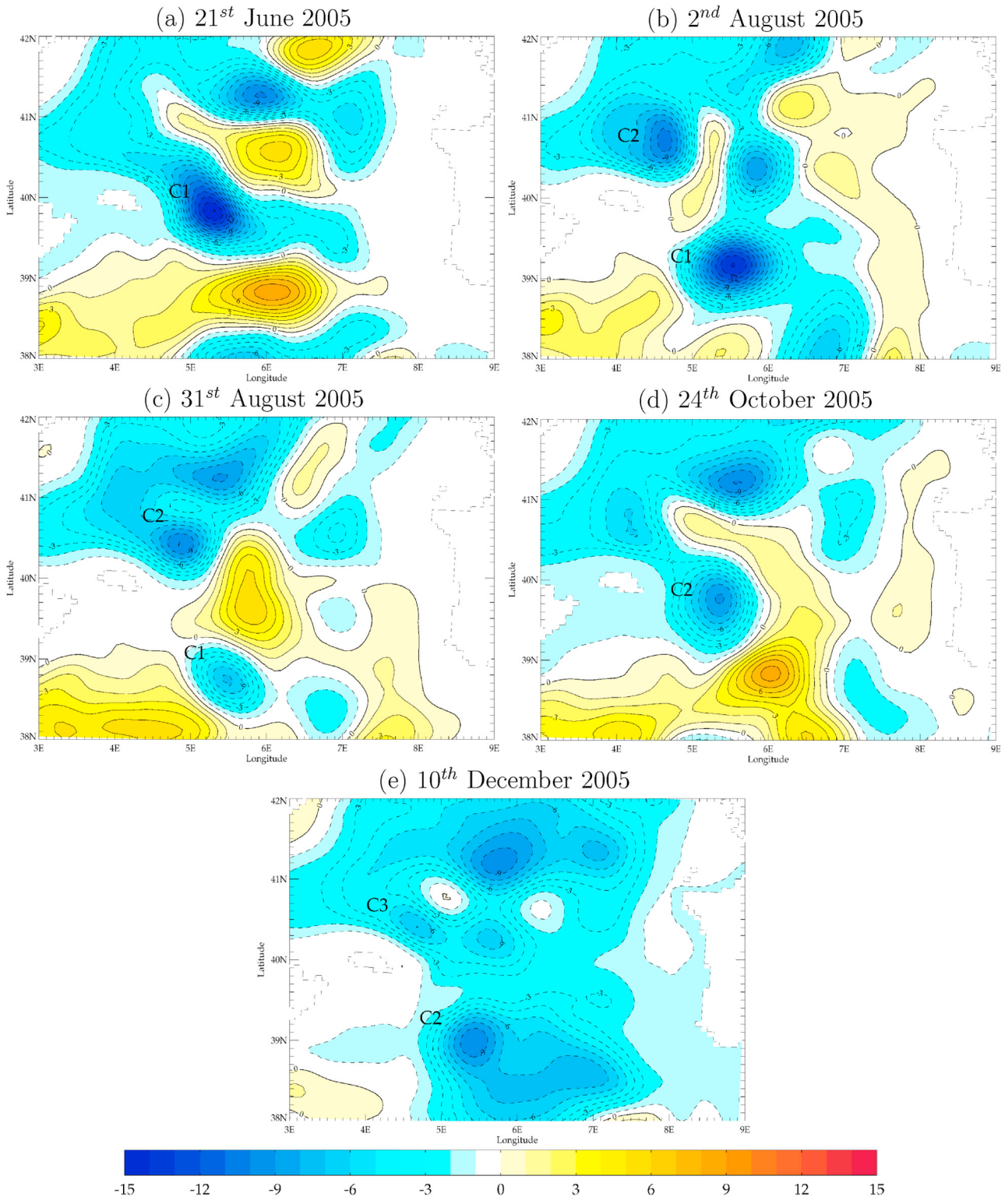

Figure 15. Daily averages of the Barotropic Stream Function (in Sv, contours every 1 Sv), in simulation MED12-ARPERA, in the center of the Western Mediterranean, for (a) the 21st June 2005, (b) the 2nd August 2005, (c) the 31st August 2005, (d) the 24th October 2005 and (e) the 10th December 2005. C1, C2 and C3 identify the three successive deep cyclones.

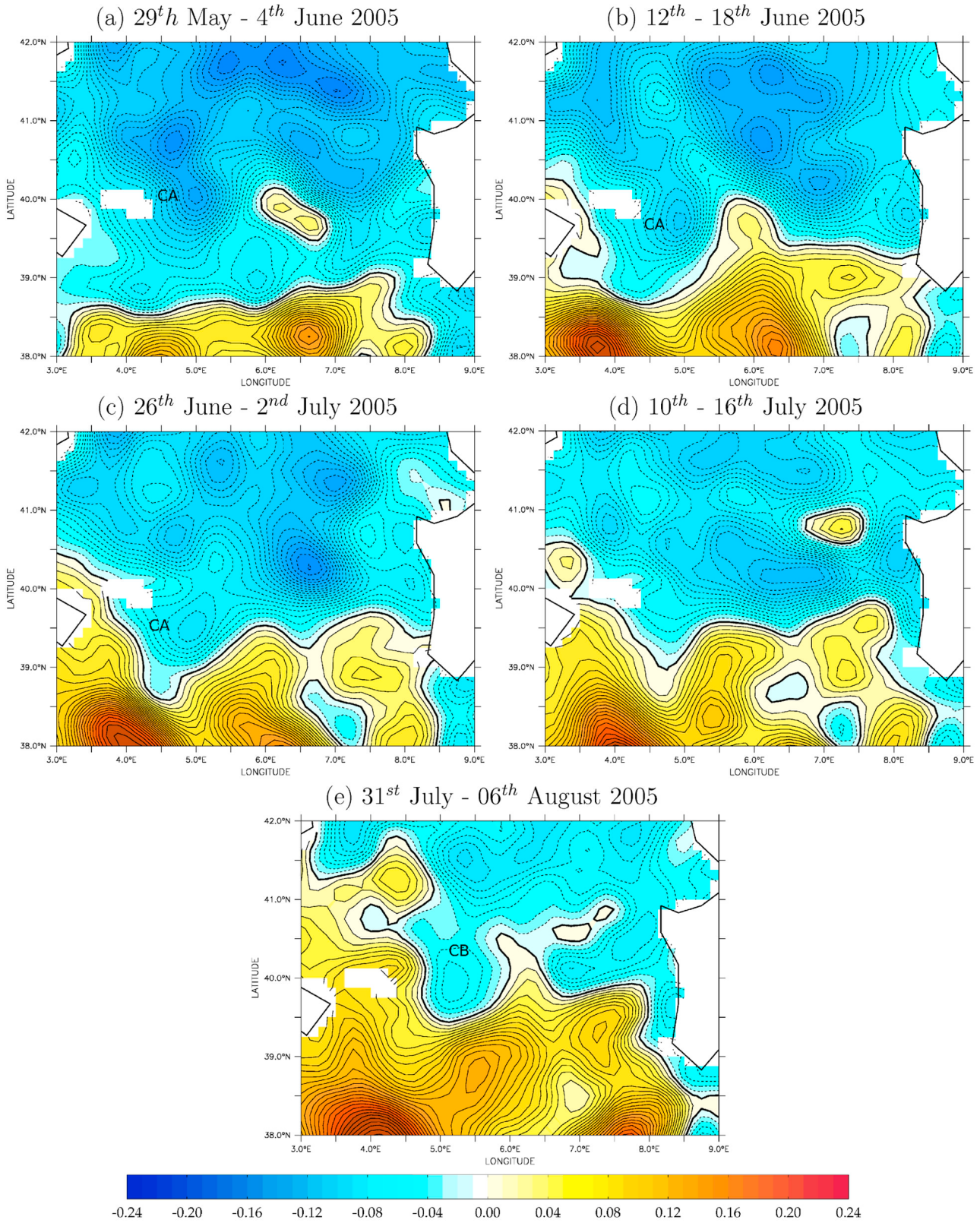

Figure 16. Weekly averages of the Sea Surface Height (in meters, contours every 0.01 m), in AVISO observations, in the center of the Western Mediterranean. CA and CB identify two successive cyclones.

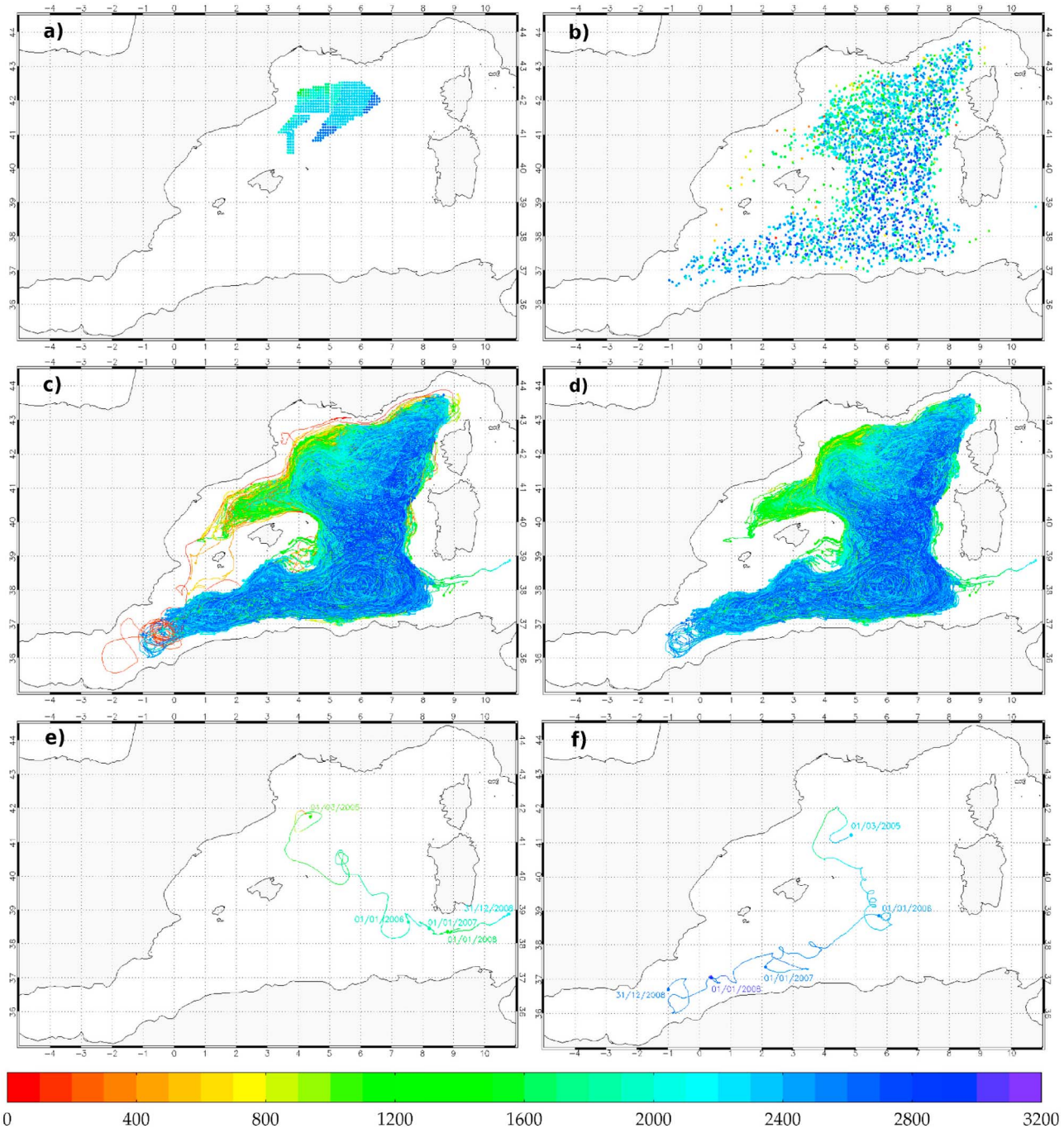

Figure 17. Overview of the main characteristics of the ARIANE simulation: (a) initial positions (1st March 2005), (b) final positions (31st December 2008), (c) all 1402-day trajectories, (d) trajectories with final positions under 1100 m, (e) easternmost trajectory and (f) westernmost trajectory. The colors indicate the depth (in meters) of positions and trajectories.

diffusion. We thus start the ARIANE simulation at the end of the deep mixing phase, that is to say on the 1st March 2005, with an ensemble of particles initialized as follow (Figure 17a): we put one particle in each ocean grid-mesh (one every 0.08° horizontally and one in each vertical level), at seven different vertical levels below 1100 m to track dense waters (1100 m, 1300 m, 1500 m, 1700 m, 2000 m, 2300 m and 2600 m), in the area corresponding to the maximal extent of the deep convection (see Figure 8). It gives an ensemble of 2839 particles. We perform an ARIANE simulation until the 31st December 2008 (1402 days of simulation). During the almost 4 years of ARIANE simulation, the particles initialized in the Gulf of Lions spread in all the Algero-Provencal, Catalan and Ligurian subbasins (Figure 17b). A few of them are uplifted to the surface layers and then carried faster, but they do not exit the Western Mediterranean (red and orange trajectories in Figure 17c). Figure 17d focuses on the particles whose final position is

deeper than 1100 m, the shallowest initial depth. The deep spreading is mainly constrained by the bathymetry. No particle reaches the Alboran subbasin (Asb in Figure 1a). Only four of them cross the Channel of Sardinia and only one propagates in the Tyrrhenian subbasin (Figure 17e). The trajectory of this latter particle, with its position at different dates, indicates that the spreading, globally southeastward, is quite fast in a first time. Then, this particle needs more than two years to cross the Channel of Sardinia. During its path, around 40.5°N−5.5°E, this particle seems to be trapped in an eddy. The particle with the westernmost trajectory (Figure 17f) shows a similar behavior: a quick southwards propagation in a first time, then toward the Strait of Gibraltar and progressively this particle goes slower (it takes 2 years to cross a distance of 3° of longitude). In the area [38°N;40°N]-[5°E;6°E], this particle seems also to be trapped in an eddy.

[49] To better characterize the fast spreading during the first year of the ARIANE simulation, we display the trajectories deeper than 1100 m by periods of two months from March 2005 to March 2006 (Figure 18). It appears that, during this first year, the spreading occurs mainly on a North-South axis, from the Gulf of Lions to the Algerian coast. Even if it is a deep propagation, it seems quite fast, since the quickest particles, which are deeper than 2000 m depth, reach the 38°N line the 1st July, i.e., after 4 months of spreading (Figure 18b). Then, the spreading on the West-East axis, toward the Strait of Gibraltar and the Channel of Sardinia, is slower, since particles first cross the 3°E line near the 1st January 2006 (Figure 18e). However, as for the comparison with satellite observations, this spreading is slower than in in-situ observations, since *Schroeder et al.* [2008] observed the presence of new WMDW off the Algerian coasts near 1°E during June 2005. The spreading toward the Channel of Sardinia is even slower, after one year no particle is in the box defined earlier in this area (Figure 18f). On all these two-month trajectories, particles are obviously carried by eddy induced circulations in the center of the Algero-Provencal subbasin (see Figures 18c, 18d and 18e). Given the dates on which these patterns occur, they can be related to the successive deep cyclonic eddies previously identified. The recirculation due to the deep eastern Algerian gyre is also noticeable on Figure 18f.

4.3.3. Discussion

[50] A deep convection event occurs in March 2005 in the simulation. New WMDW is formed in large volume. With a noticeable signature in density, we track this water mass until the southern part of the Algero-Provencal subbasin (APsb in Figure 1a). In the simulation, the Eulerian and Lagrangian approaches give different estimates of this new WMDW transport time toward the southern boundaries of the Algero-Provencal subbasin (the Channel of Sardinia and the Strait of Gibraltar). It can be assumed that the Eulerian approach includes diffusive and mixing processes whereas the Lagrangian approach gives an approximation of only the advective transport time. In the area at the western entrance of the Channel of Sardinia, changes of the deep water thermohaline characteristics appear 9 to 10 months after the convection event whereas in the ARIANE simulation, particles need more than one year to propagate toward this area. Thus, in the southeastern part of the Algero-Provencal subbasin, new WMDW characteristics are carried faster when diffusion and mixing are taken into account than through advection only. On the contrary, particles in the ARIANE simulation arrive in the western Algerian subbasin 8 months after the convection event, while we showed that the deep thermohaline characteristics changed there 12 to 13 months after winter 2005. Thus, in the southwestern part of the Algero-Provencal subbasin, advection alone carries quicker the new WMDW characteristics than when diffusion and mixing are also considered.

[51] The main pathway of spreading for the WMDW in the southern part of the Algero-Provencal subbasin should be constrained by the bathymetry and the Coriolis force [*Millot*, 1999]. It means that the current along the continental slope of the Balearic Islands is the favorite advective path for the spreading of WMDW. Thus, the effect of the main advective spreading (i.e., without the eddy circulation) tends to propagate WMDW toward the Strait of Gibraltar rather than toward the Channel of Sardinia. But a part of it is trapped into the eastern Algerian gyre by closed f/H isocontours constraint [*Testor et al.*, 2005], where f is the planetary vorticity and H the water depth. On the contrary, we showed that the deep eddy circulation south of the Balearic Islands toward the center of the Algerian subbasin is able to transport WMDW characteristics to the east toward the Channel of Sardinia. Then they disappeared by mixing and diffusion in the interior of the Algerian subbasin. We can thus say that the deep eddy circulation, in comparison to the main advective path alone, accelerates the spreading of the new WMDW characteristics through diffusion and mixing toward the Channel of Sardinia and reduces the available quantity of WMDW which can reach the Strait of Gibraltar.

[52] We identified a southwards and southeastward direction of propagation of deep eddies carrying WMDW. This is in agreement with the findings of *Testor and Gascard* [2003] and *Testor and Gascard* [2006], who showed that numerous eddies, both anticyclonic and cyclonic, export WMDW far away from the convection area and with the same direction of propagation (southwards and southeastward). However, as they are submesoscale features with a typical size of 5–10 km, they cannot be reproduced in our model. Nevertheless, deep cyclonic eddies with a larger size have already been observed, since *Send et al.* [1999] mentioned the observation of a large cyclonic eddy in the Algerian subbasin (near 38°N, 6.5°E). Concerning modeling studies, *Demirov and Pinardi* [2007] simulated a similar propagation of cyclonic eddies with a diameter of 80–100 km from the North to the South of the Algero-Provencal subbasin. With a higher resolution coastal model (horizontal resolution about 3 km), *Herrmann et al.* [2008] identified mesoscale eddies with a typical size between 25 and 50 km as responsible of one third of the export of dense water away from the convection area in the open-sea part of the Gulf of Lions. But, as their model do not extend more south than the Minorca-Sardinia line, they were not able to quantify the further propagation in the Algerian subbasin. MED12, with an horizontal resolution between 6 and 8 km, is able to resolve the mesoscale processes, the first Rossby radius being equal in average to about 10 km in the Mediterranean Sea. Nevertheless, as ocean circulation models like MED12 are able to represent only processes whose spatial scale (diameter) is larger than 5–6 times their

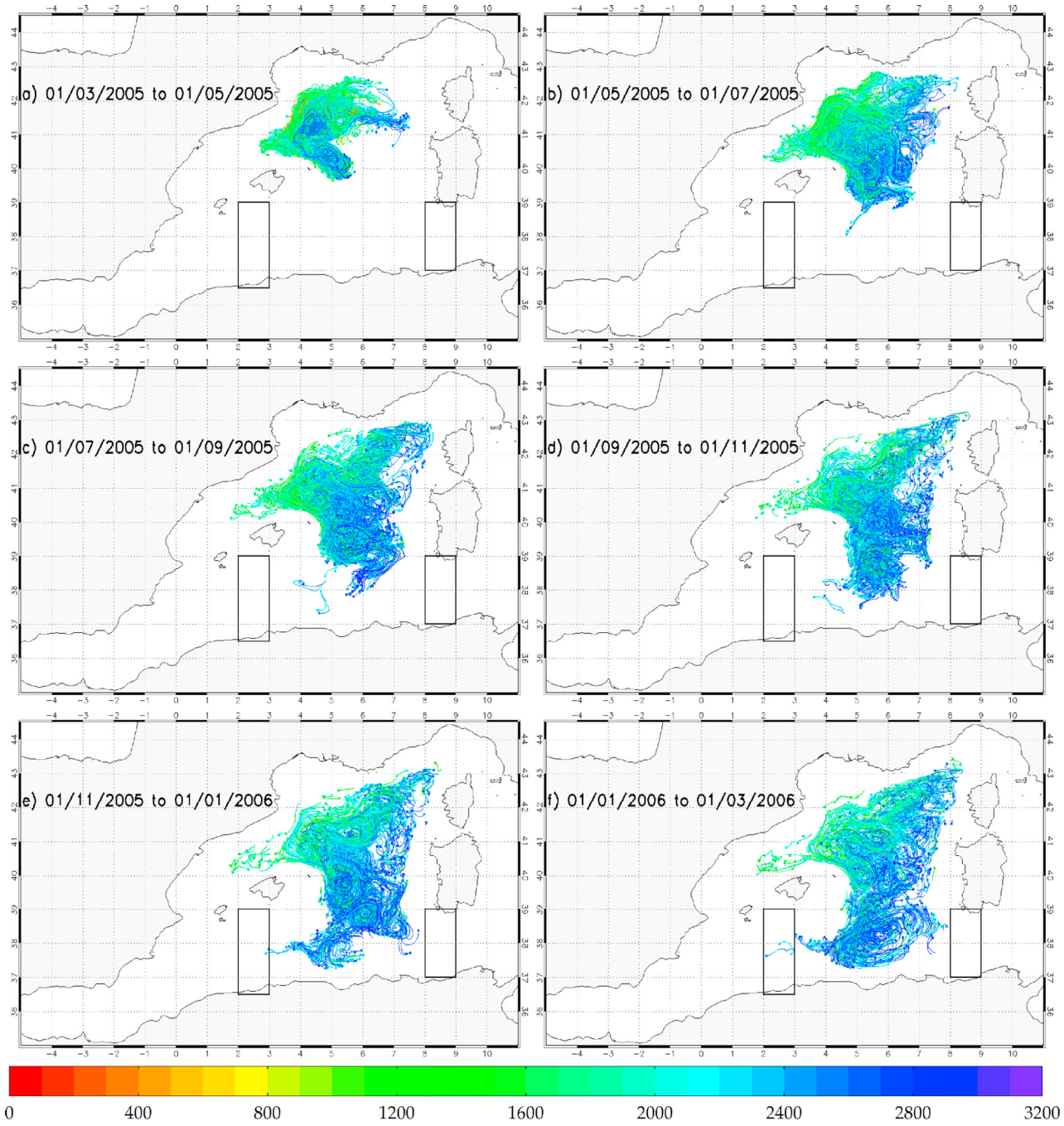

Figure 18. Trajectories deeper than 1100 m during the first year of the ARIANE simulation: (a) from the 1st March 2005 to the 1st May 2005, (b) from the 1st May 2005 to the 1st July 2005, (c) from the 1st July 2005 to the 1st September 2005, (d) from the 1st September 2005 to the 1st November 2005, (e) from the 1st November 2005 to the 1st January 2006 and (f) from the 1st January 2006 to the 1st March 2006. The colors indicates the depth (in meters) of positions and trajectories. The rectangles correspond to the boxes of the θ-S diagrams of Figure 10.

horizontal resolution, MED12 is able to simulate only eddies whose horizontal scale is larger than 40 km (which is probably a size between meso- and sub-meso scales). We can thus assume that increasing the horizontal resolution of our model would maybe lower the size of the mesoscale eddies involved in the deep spreading of the WMDW, and also probably improve the modeling of the deep water advection time. However, our first attempt to simulate the winter 2005 deep water formation within a 4-year simulation of the whole Mediterranean Sea at 1/36° ORCA resolution (MED36 configuration with a 2.5 km horizontal resolution) tends to moderate this assessment, as the thick barotropic cyclonic eddies we identified here with MED12 still have an horizontal extent larger than 75 km in the

MED36 configuration [*Beuvier*, 2011]. It will be the subject of following studies.

[53] The volume of new WMDW formed in the simulation is estimated to be lower by about 1.5 Sv compared to what was deduced from in-situ observations. This leads to a potential loss of WMDW along its spreading pathes by mixing and diffusion relatively higher and quicker than in the reality. Moreover, the deep layers in the model are relatively thick at the Algero-Provencal subbasin floor (about 300 m thick at 2400 m depth). This explains why the deep velocity is relatively slow in the model compared to observations. Considering these two points, it can be inferred that the real transport time would be smaller than our model estimates. Indeed, we deduced from the comparison with satellite observations that it takes 2 months for surface cyclonic eddies to pass from the southern part of the Gulf of Lions toward the Algerian subbasin, and *Schroeder et al.* [2008] observed new WMDW characteristics in the Algerian subbasin 4 months after the convection event of winter 2005. Nevertheless, the model approach allows to draw a 4D picture of the deep water spreading process after the intense convection event of winter 2005, which has never been done before, to our knowledge, in a modeling study for this typical year. In particular, we showed that deep cyclonic eddies with a typical size of about 100 km wide and more than 1500 m thick, are mainly responsible of the fast WMDW spreading process. It allowed us to complete the view given by in-situ observations, which are by definition sparse in space and time.

5. Conclusion and Outlook

[54] In this work, we have studied the spreading of the WMDW formed in the Gulf of Lions during winter 2005 by using MED12, an eddy-resolving model of the Mediterranean Sea at 1/12° of horizontal resolution (6–8 km). A simulation of the 1998–2008 period has been performed, with a daily atmospheric forcing from ARPERA, a high-resolution dynamical downscaling of ECMWF products. The use of new state-of-the-art parameterizations has been validated with respect to satellite observations and gridded data set deduced from in-situ observations. The use of a new Atlantic sea level condition allows the simulation to well reproduce the variability of the net water flux through the Strait of Gibraltar and of the SSH in the Mediterranean Sea. Then, we analyzed the simulation in terms of interannual variability in the Western Mediterranean and of WMDW formation rate in 2005.

[55] We have shown that the strong convection event of winter 2005 in the Gulf of Lions was well reproduced in the simulation. The formation of a substantial volume of WMDW with a well marked density signature allowed its tracking in the Western Mediterranean. It induced an important uplift of the isopycnal surfaces, with an amplitude in agreement with in-situ observations. We identified several deep cyclones that successively trap and carry WMDW southwards. The occurrence of such cyclonic eddies is realistic with respect to satellite observations. The comparison of Eulerian and Lagrangian approaches highlights the role of these cyclones in spreading the thermohaline characteristics of the WMDW toward the Channel of Sardinia.

[56] Some aspects in the simulation could be improved. We obtained a higher WMDW formation rate in winter 2005 than in previous modeling works, but it is still smaller than the formation rate deduced from in-situ observations. In addition, the new WMDW formed in the model is too cold and not salty enough with respect to these observations. Its southwards propagation is also too slow if directly compared with in-situ observations and indirectly with satellite observations.

[57] Future work will thus focus on the effect of increasing the horizontal resolution (with a global Mediterranean model at 1/36° or with embedded coastal models) on the scale of the eddies responsible for a part of the WMDW spreading. The vertical resolution of the model will also be improved, especially near the sea bottom, to better reproduce the deep water mass propagation. Atmospheric forcing at higher resolution (about 12 km [see *Herrmann et al.*, 2011]), will also be used, probably allowing an enhancement of the dense water formation rate. Longer simulations [*Beuvier*, 2011] will help to have better oceanic conditions before winter 2005, as *Beuvier et al.* [2010] and *Herrmann et al.* [2010] did, but with an eddy-permitting model, and also to assess the place of the winter 2005 deep convection event in the long-term variability of the Gulf of Lions and of the entire Mediterranean Sea.

[58] **Acknowledgments.** We thank the three anonymous reviewers for their fruitful comments and discussions, which helped us to focus on the main results of this study. The numerical work was supported by the Groupe de Mission Mercator Coriolis (GMMC). This work was granted access to the HPC resources of IDRIS (Institut du Développement et des Ressources en Informatique Scientifique) of the Centre National de la Recherche Scientifique (CNRS) under allocation 2010 and 2011 (project number 010227) made by Grand Equipement National de Calcul Intensif (GENCI). The financial support of J. Beuvier's Ph.D was provided by Météo-France. We thank Michel Déqué from Météo-France for running the ARPERA simulation with ARPEGE-Climate. The realization of GLORYS1 global ocean reanalysis had the benefit of the grants that Groupe Mission Mercator Coriolis, Mercator Ocean, and INSU-CNRS attributed to the GLORYS project, and the support of the European Union FP7 via the MYOCEAN project; computations for GLORYS1 were performed with the support of Météo-France HPC Center. We thank Bruno Levier from Mercator Océan for gathering the bathymetry products. We acknowledge the GEBCO-08 Grid, version 20081212, http://www.gebco.net, for providing the GEBCO-08 bathymetry. The altimeter products were produced by Ssalto/Duacs and distributed by AVISO, with support from Cnes (http://www.aviso.oceanobs.com/duacs/). This work is a contribution to the HyMeX international program on the study of the water cycle in the Mediterranean area.

References

Arakawa, A., and V. R. Lamb (1981), A potential energy and enstrophy conserving scheme for the shallow water equations, *Mon. Weather Rev.*, *109*, 18–36.

Artale, V., D. Iudicone, R. Santoleri, V. Rupolo, S. Marullo, and F. D'Ortenzio (2002), Role of surface fluxes in ocean general circulation models using satellite sea surface temperature: Validation of and sensitivity to the forcing frequency of the Mediterranean thermohaline circulation, *J. Geophys. Res.*, *107*(C8), 3120, doi:10.1029/2000JC000452.

Barnier, B., L. Siefridt, and P. Marchesiello (1995), Thermal forcing for a global ocean circulation model using a three-year climatology of ECMWF analyses, *J. Mar. Syst.*, *6*, 363–380.

Barnier, B., et al. (2006), Impact of partial steps and momentum advection schemes in a global ocean circulation model at eddy-permitting resolution, *Ocean Dyn.*, *56*, 543–567.

Baschek, B., U. Send, J. Garcia Lafuente, and J. Candela (2001), Transport estimates in the Strait of Gibraltar with a tidal inverse model, *J. Geophys. Res.*, *112*, 31,033–31,044.

Béranger, K., L. Mortier, and M. Crépon (2005), Seasonal variability of water transport through the Straits of Gibraltar, Sicily and Corsica,

derived from a high-resolution model of the Mediterranean circulation, *Prog. Oceanogr.*, *66*, 341–364.

Béranger, K., P. Testor, and M. Crépon (2009), Modelling water mass formation in the Gulf of Lion (Mediterranean Sea), in *Dynamics of Mediterranean Deep Waters*, *CIESM Workshop Monogr.*, vol. 38, edited by F. Briand, pp. 91–100, Mediter. Sci. Comm., Monaco.

Béranger, K., et al. (2010), Impact of the spatial distribution of the atmospheric forcing on water mass formation in the Mediterranean Sea, *J. Geophys. Res.*, *115*, C12041, doi:10.1029/2009JC005648.

Berné, S., D. Carré, B. Loubrieu, J.-P. Mazé, L. Morvan, and A. Normand (2004), Le golfe du Lion - Carte morpho-bathymétrique, Ifremer, Brest, France.

Béthoux, J. (1979), Budgets of the Mediterranean Sea. Their dependence on the local climate and on the characteristics of the Atlantic waters, *Oceanol. Acta*, *2*(2), 157–163.

Beuvier, J. (2011), Modelling the long-term variability of circulation and water masses in the Mediteranean Sea: Impacts of the ocean-atmosphere exchanges [in French], PhD thesis, 290 pp., Mech. Dep., Ecole Polytech., Palaiseau, France.

Beuvier, J., F. Sevault, M. Herrmann, H. Kontoyiannis, W. Ludwig, M. Rixen, E. Stanev, K. Béranger, and S. Somot (2010), Modeling the Mediterranean Sea interannual variability during 1961–2000: Focus on the Eastern Mediterranean Transient, *J. Geophys. Res.*, *115*, C08017, doi:10.1029/2009JC005950.

Blanke, B., and P. Delecluse (1993), Low frequency variability of the tropical Atlantic Ocean simulated by a general circulation model with mixed layer physics, *J. Phys. Oceanogr.*, *23*, 1363–1388.

Blanke, B., and S. Raynaud (1997), Kinematics of the Pacific Equatorial Undercurrent: An Eulerian and Lagrangian approach from GCM results, *J. Phys. Oceanogr.*, *27*(6), 1038–1053.

Boukthir, M., and B. Barnier (2000), Seasonal and inter-annual variations in the surface freshwater flux in the Mediterranean Sea from the ECMWF re-analysis project, *J. Mar. Syst.*, *24*, 343–354.

Bozec, A., P. Bouruet-Aubertot, D. Iudicone, and M. Crépon (2008), Impact of penetrative solar radiation on the diagnosis of water mass transformation in the Mediterranean Sea, *J. Geophys. Res.*, *113*, C06012, doi:10.1029/2007JC004606.

Bryden, H. L., and T. H. Kinder (1991), Steady two-layer exchange through the Strait of Gibraltar, *Deep Sea Res., Part A*, *38*, 445–463.

Bryden, H. L., J. Candela, and T. H. Kinder (1994), Exchange through the Strait of Gibraltar, *Prog. Oceanogr.*, *33*, 201–248.

Canals, M., P. Puig, X. Durrieu de Madron, S. Heussner, A. Palanques, and J. Fabres (2006), Flushing submarine canyons, *Nature*, *444*, 354–357.

Candela, J. (2001), The Mediterranean water and the global circulation, in *Observing and Modelling the Global Ocean*, edited by G. Siedler, J. Church, and J. Gould, pp. 419–429, Academic, San Diego, Calif.

Castellari, S., N. Pinardi, and K. Leaman (2000), Simulation of water mass formation processes in the Mediterranean Sea: Influence of the time frequency of the atmospheric forcing, *J. Geophys. Res.*, *105*(C10), 24,157–24,181, doi:10.1029/2000JC900055.

CLIPPER Project Team (1999), Modélisation à haute résolution de la circulation dans l'océan Atlantique forcée et couplée océan-atmosphère, *Sci. Tech. Rep. CLIPPER-R3-99*, Ifremer, Brest, France.

Demirov, E. K., and N. Pinardi (2007), On the relationship between the water mass pathways and eddy variability in the western Mediterranean Sea, *J. Geophys. Res.*, *112*, C02024, doi:10.1029/2005JC003174.

Déqué, M., and J. Piedelievre (1995), High resolution climate simulation over Europe, *Clim. Dyn.*, *11*, 321–339.

Fernàndez, V., D. E. Dietrich, R. L. Haney, and J. Tintoré (2005), Mesoscale, seasonal and interannual variability in the Mediterranean Sea using a numerical ocean model, *Prog. Oceanogr.*, *66*, 321–340, doi:10.1016/j.pocean.2004.07.010.

Ferry, N., L. Parent, G. Garric, B. Barnier, N. C. Jourdain, and the Mercator Ocean team (2010), Mercator global eddy permitting ocean reanalysis GLORYS1V1: Description and results, *Mercator Ocean Q. Newsl.*, *36*, 15–28.

Font, J., P. Puig, J. Salat, A. Palanques, and M. Emelianov (2007), Sequence of hydrographic changes in NW Mediterranean deep water due to the exceptional winter of 2005, *Sci. Mar.*, *71*(2), 339–346.

Herrmann, M. J., and S. Somot (2008), Relevance of ERA40 dynamical downscaling for modeling deep convection in the Mediterranean Sea, *Geophys. Res. Lett.*, *35*, L04607, doi:10.1029/2007GL032442.

Herrmann, M., S. Somot, F. Sevault, C. Estournel, and M. Déqué (2008), Modeling the deep water convection in the northwestern Mediterranean Sea using an eddy-permitting and an eddy-resolving model: Case study of winter 1986–1987, *J. Geophys. Res.*, *113*, C04011, doi:10.1029/2006JC003991.

Herrmann, M., F. Sevault, J. Beuvier, and S. Somot (2010), What induced the exceptional 2005 convection event in the northwestern Mediterranean basin? Answers from a modeling study, *J. Geophys. Res.*, *115*, C12051, doi:10.1029/2010JC006162.

Herrmann, M., S. Somot, S. Calmanti, C. Dubois, and F. Sevault (2011), Representation of spatial and temporal variability of daily wind speed and of intense wind events over the Mediterranean Sea using dynamical downscaling: Impact of the regional climate model configuration, *Nat. Haz. Earth Syst. Sci.*, *11*, 1983–2001, doi:10.5194/nhess-11-1983-2011.

Ingleby, B., and M. Huddleston (2007), Quality control of ocean temperature and salinity profiles—Historical and real-time data, *J. Mar. Syst.*, *65*, 158–175, doi:10.1016/j.jmarsys.2005.11.019.

Koch-Larrouy, A., G. Madec, P. Bouruet-Aubertot, T. Gerkema, L. Bessières, and R. Molcard (2007), On the transformation of Pacific Water into Indonesian Throughflow Water by internal tidal mixing, *Geophys. Res. Lett.*, *34*, L04604, doi:10.1029/2006GL028405.

Lafuente, J. G., J. Delgado, J. M. Vargas, M. Vargas, F. Plaza, and T. Sarhan (2002), Low frequency variability of the exchanged flows through the Strait of Gibraltar during CANIGO, *Deep Sea Res., Part II*, *49*, 4051–4067.

Lebeaupin Brossier, C., K. Béranger, C. Deltel, and P. Drobinski (2011), The Mediterranean response to different space-time resolution atmospheric forcings using perpetual mode sensitivity simulations, *Ocean Modell.*, *36*, 1–25, doi:10.1016/j.ocemod.2010.10.008.

Lebeaupin Brossier, C., K. Béranger, and P. Drobinski (2012), Sensitivity of the northwestern Mediterranean Sea coastal and thermohaline circulations simulated by the 1/12°-resolution ocean model NEMO-MED12 to the spatial and temporal resolution of atmospheric forcing, *Ocean Modell.*, *43–44*, 94–107, doi:10.1016/j.ocemod.2011.12.007.

Levitus, S., J. Antonov, and T. Boyer (2005), Warming of the world ocean, 1955–2003, *Geophys. Res. Lett.*, *32*, L02604, doi:10.1029/2004GL021592.

López-Jurado, J.-L., C. González-Pola, and P. Vélez-Belchi (2005), Observation of an abrupt disruption of the long-term warming trend at the Balearic Sea, western Mediterranean Sea, in summer 2005, *Geophys. Res. Lett.*, *32*, L24606, doi:10.1029/2005GL024430.

Ludwig, W., E. Dumont, M. Meybeck, and S. Heussner (2009), River discharges of water and nutrients to the Mediterranean and Black Sea: Major drivers for ecosystem changes during past and future decades?, *Prog. Oceanogr.*, *80*, 199–217.

Lyard, F., F. Lefevre, T. Letellier, and O. Francis (2006), Modelling the global ocean tides: Modern insights from FES2004, *Ocean Dyn.*, *56*(5–6), 394–415, doi:10.1007/s10236-006-0086-x.

Macdonald, A. M., J. Candela, and H. L. Bryden (1994), An estimate of the net heat transport through the Strait of Gibraltar, in *Seasonal and Interannual Variability of the Western Mediterranean Sea Coastal and Estuarine Studies, Coastal Estuarine Stud.*, vol. 46, edited by P. E. La Violette et al., pp. 13–32, AGU, Washingtion, D. C.

Madec, G., and the NEMO Team (2008), *NEMO Ocean Engine*, *Note Pôle Modél. 27*, Inst. Pierre-Simon Laplace, Paris.

Madec, G., F. Lott, P. Delecluse, and M. Crépon (1996), Large-scale preconditioning of deep-water formation in the northwestern Mediterranean Sea, *J. Phys. Oceanogr.*, *26*, 1393–1408.

Mantziafou, A., and A. Lascaratos (2004), An eddy resolving numerical study of the general circulation and deep-water formation in the Adriatic Sea, *Deep Sea Res., Part I*, *51*, 921–952, doi:10.1016/j.dsr.2004.03.006.

Mariotti, A., N. Struglia, N. Zeng, and K.-M. Lau (2002), The hydrological cycle in the Mediterranean region and implications for the water budget of the Mediterranean Sea, *J. Clim.*, *15*, 1674–1690.

Marshall, J., and F. Schott (1999), Open-ocean convection: Observations, theory, and models, *Rev. Geophys.*, *37*(1), 1–64.

MEDAR/MEDATLAS Group (2002), *MEDAR/MEDATLAS 2002 Database, Mediterranean and Black Sea Database of Temperature Salinity and Bio-chemical Parameters* [CD-ROM], IFREMER, Brest, France.

Medimap Group (2005), Morpho-bathymetry of the Mediterranean Sea, scale 1/2000000, CIESM/Ifremer, Brest, France.

MEDOC Group (1970), Observation of formation of deep water in the Mediterranean Sea, 1969, *Nature*, *227*, 1037–1040.

Millot, C. (1999), Circulation in the western Mediterranean Sea, *J. Mar. Syst.*, *20*, 423–442.

Millot, C., and I. Taupier-Letage (2005), Circulation in the Mediterranean Sea, in *The Handbook of Environmental Chemistry*, vol. 5, pp. 29–66, Springer, New York, doi:10.1007/b107143.

Pascual, A., B. Buongiorno Nardelli, G. Larnicol, M. Emelianov, and D. Gomis (2002), A case of an intense anticyclonic eddy in the Balearic Sea (western Mediterranean), *J. Geophys. Res.*, *107*(C11), 3183, doi:10.1029/2001JC000913.

Pascual, A., M.-I. Pujol, G. Larnicol, P.-Y. Le Traon, and M.-H. Rio (2007), Mesoscale mapping capabilities of multisatellite altimeter missions: First results with real data in the Mediterranean Sea, *J. Mar. Syst.*, *65*, 190–211, doi:10.1016/j.jmarsys.2004.12.004.

Pinardi, N., and E. Masetti (2000), Variability of the large scale general circulation of the Mediterranean Sea from observations and modelling: A review, *Palaeogeogr. Palaeoclimatol. Palaeoecol.*, *158*, 153–173.

Pinot, J.-M., J. L. López-Jurado, and M. Riera (2002), The CANALES experiment (1996–1998). Interannual, seasonal, and mesoscale variability of the circulation in the Balearic Channels, *Prog. Oceanogr.*, *55*, 335–370.

Pujol, M.-I., and G. Larnicol (2005), Mediterranean Sea eddy kinetic energy variability from 11 years of altimetric data, *J. Mar. Syst.*, *58*, 121–142.

Reynolds, R. W., N. A. Rayner, T. M. Smith, D. C. Stokes, and W. Wang (2002), An improved in situ and satellite SST analysis for climate, *J. Clim.*, *15*, 1609–1625.

Rio, M.-H., P.-M. Poulain, A. Pascual, E. Mauri, G. Larnicol, and R. Santoleri (2007), A mean dynamic topography of the Mediterranean Sea computed from altimetric data, in-situ measurements and a general circulation model, *J. Mar. Syst.*, *65*, 484–508, doi:10.1016/j.jmarsys.2005.02.006.

Roether, W., B. Klein, B. B. Manca, A. Theocharis, and S. Kioroglou (2007), Transient eastern Mediterranean deep waters in response to the massive dense-water output of the Aegean Sea in the 1990s, *Prog. Oceanogr.*, *74*, 540–571.

Roullet, G., and G. Madec (2000), Salt conservation, free surface, and varying levels: a new formulation for ocean general circulation models, *J. Geophys. Res.*, *105*(C10), 23,927–23,942.

Sanchez-Gomez, E., S. Somot, S. A. Josey, C. Dubois, N. Elguindi, and M. Déqué (2011), Evaluation of Mediterranean Sea water and heat budgets simulated by an ensemble of high resolution regional climate models, *Clim. Dyn.*, *37*(9–10), 2067–2086, doi10.1007/s00382-011-1012-6.

Sannino, G., A. Bargali, and V. Artale (2004), Numerical modeling of the semidiurnal tidal exchange through the Strait of Gibraltar, *J. Geophys. Res.*, *109*, C05011, doi:10.1029/2003JC002057.

Sannino, G., M. Herrmann, A. Carillo, V. Rupolo, V. Ruggiero, V. Artale, and P. Heimbach (2009), An eddy-permitting model of the Mediterranean Sea with a two-way grid refinement at the Strait of Gibraltar, *Ocean Modell.*, *30*, 56–72, doi:10.1016/j.ocemod.2009.06.002.

Schott, F., M. Visbeck, U. Send, J. Fischer, L. Stramma, and Y. Desaubies (1996), Observations of deep convection in the Gulf of Lions, northern Mediterranean, during the winter of 1991/1992, *J. Phys. Oceanogr.*, *26*(4), 505–524.

Schröder, K., G. P. Gasparini, M. Tangherlini, and M. Astraldi (2006), Deep and intermediate water in the western Mediterranean under the influence of the Eastern Mediterranean Transient, *Geophys. Res. Lett.*, *33*, L21607, doi:10.1029/2006GL027121.

Schroeder, K., A. Ribotti, M. Borghini, R. Sorgente, A. Perilli, and G. P. Gasparini (2008), An extensive western Mediterranean deep water renewal between 2004 and 2006, *Geophys. Res. Lett.*, *35*, L18605, doi:10.1029/2008GL035146.

Send, U., J. Font, G. Krahmann, M. Millot, M. Rhein, and J. Tintoré (1999), Recent advances in observing the physical oceanography of the western Mediterranean Sea, *Prog. Oceanogr.*, *44*, 37–64.

Simmons, A., and J. Gibson (2000), The ERAB-40 project plan, *ECMWF ERA-40 Proj. Rep. Ser. 1*, Eur. Cent. for Medium-Range Weather Forecasts, Reading, U. K.

Smith, R. O., H. L. Bryden, and K. Stansfield (2008), Observations of new western Mediterranean deep water formation using Argo floats 2004−2006, *Ocean Sci.*, *4*, 133–149.

Somot, S., F. Sevault, and M. Déqué (2006), Transient climate change scenario simulation of the Mediterranean Sea for the twenty-first century using a high-resolution ocean circulation model, *Clim. Dyn.*, *27*, 851–879.

Soto-Navarro, J., F. Criado-Aldeanueva, J. García-Lafuente, and A. Sánchez-Román (2010), Estimation of the Atlantic inflow through the Strait of Gibraltar from climatological and in situ data, *J. Geophys. Res.*, *115*, C10023, doi:10.1029/2010JC006302.

Stanev, E. V., and E. L. Peneva (2002), Regional sea level response to global climatic change: Black Sea examples, *Global Planet. Changes*, *32*, 33–47.

Testor, P., and J.-C. Gascard (2003), Large scale spreading of deep waters in the western Mediterranean Sea by submesoscale coherent eddies, *J. Phys. Oceanogr.*, *33*, 75–87.

Testor, P., and J.-C. Gascard (2006), Post-convection spreading phase in the northwestern Mediterranean Sea, *Deep Sea Res., Part I*, *53*, 869–893, doi:10.1016/j.dsr.2006.02.004.

Testor, P., U. Send, J.-C. Gascard, C. Millot, I. Taupier-Letage, and K. Béranger (2005), The mean circulation of the southwestern Mediterranean Sea: Algerian Gyres, *J. Geophys. Res.*, *110*, C11017, doi:10.1029/2004JC002861.

THETIS Group (1994), Open-ocean deep convection explored in the Mediterranean, *Eos Trans. AGU*, *75*(19), 217.

Tonani, M., N. Pinardi, S. Dobricic, I. Pujol, and C. Fratianni (2008), A high-resolution free-surface model of the Mediterranean Sea, *Ocean Sci.*, *4*, 1–14.

Tsimplis, M. N., and H. L. Bryden (2000), Estimation of the transport through the Strait of Gibraltar, *Deep Sea Res., Part I*, *47*, 2219–2242.

Vargas-Yáñez, M., F. Plaza, J. García-Lafuente, T. Sarhan, J. M. Vargas, and P. Vélez-Belchi (2002), About the seasonal variability of the Alboran Sea circulation, *J. Mar. Syst.*, *35*, 229–248.

Vörösmarty, C., B. Fekete, and B. Tucker (1996), Global river discharge database, RivDis, technical document, UNESCO, Paris.